DIAGENESIS AND RESERVOIR QUALITY OF THE UPPER PALEOCENE SUCCESSION, WESTERN DAHRA PLATFORM, SIRT BASIN, LIBYA

Ibrahim E. Elkanouni[1] and Maurice E. Tucker[2]

Abstract: The Selandian/Thanetian succession in the western Sirt Basin, Libya, is mainly composed of carbonates with lesser amounts of shale. They were deposited on a platform-homoclinal ramp with inner, mid and outer ramp facies, each with distinctive microfacies, ranging from mud-supported to grain-dominated carbonates. Two phases of dissolution, near-surface and burial, affected the late Paleocene succession. Marine and meteoric cements are minor, but early dolomite is locally developed. Burial compaction is widespread, associated with calcite and dolomite cements. The average $\delta^{13}C$ values in the Dahra and Zelten/Harash formations are 2.3‰ and 3.2‰, respectively. Both show no significant change up through the section, which suggests a stable carbon isotope composition of seawater through Selandian/Thanetian time, with little latter diagenetic alteration through organic matter decomposition. On the other hand, the $\delta^{18}O$ data show more negative values than most signatures reported for the Paleocene; this is largely the result of meteoric water influx and/or burial cementation-neomorphism under increasing temperature; this is supported by fluid-inclusion results. The best porosity is recorded in grainstones of the Dahra Formation, whereas, the Zelten and Harash formations have much lower porosity. The highest porosity is developed in bioclastic foraminiferal grainstone, bioclastic foraminiferal packstone-packstone/grainstone facies and, less important, foraminiferal nummulitic packstone. The porosity evolution in the Selandian/Thanetian succession is controlled by original depositional texture and subsequent diagenesis.

Keywords: Selandian/Thanetian, Sirt Basin, facies, diagenesis, porosity, stable isotopes, fluid inclusions.

INTRODUCTION

The Sirt Basin (Fig. 1) developed through inter- and intra-plate movements resulting from the relative motion of the American, African and Eurasian plates during the opening of the Atlantic Ocean and the development of the Mediterranean on the foreland of the African Plate (Anketell, 1996). The Paleocene succession in the Sirt Basin is dominated for the most part by shallow-water carbonates deposited in restricted shallow-platform to open-marine environments. The carbonate platforms usually have a clearly definable ramp margin with more argillaceous sediments occurring in the deeper-water areas.

Diagenesis of carbonate sediments includes obvious processes such as cementation to produce limestones and dissolution to form cave systems but it also includes more subtle processes such as the development of microporosity and changes in trace element and isotopic signatures. Diagenetic changes can begin on the seafloor, even as the grains are still being moved around, or little may happen until significant burial when overburden pressure has increased, or pore-fluid chemistry has changed, so that reactions are then induced within the sediments (Tucker and Wright, 1990; Flügel and Munnecke, 2010; James and Jones, 2015). Major controls on the diagenesis of carbonates are the composition and mineralogy of the sediment, the pore-fluid chemistry and flow rates, geological history of the sediment in terms of sea-level change and prevailing climate, and burial and uplift (see Tucker, 1993).

After deposition and during their burial history, the Selandian/Thanetian carbonate rocks in the western Sirt Basin were affected by a range of diagenetic processes. These led to the development of porosity at particular levels which has resulted in these rocks becoming important reservoirs for hydrocarbons.

The main objectives of this paper are to describe and interpret the post-depositional processes that have affected the Paleocene succession in the western

[1] *Libyan Petroleum Institute, Km 7, Gergarish Road, P. O. Box 6431, Tripoli, Libya.*
[2] *School of Earth Sciences, University of Bristol, Bristol BS8 3RW, UK.*

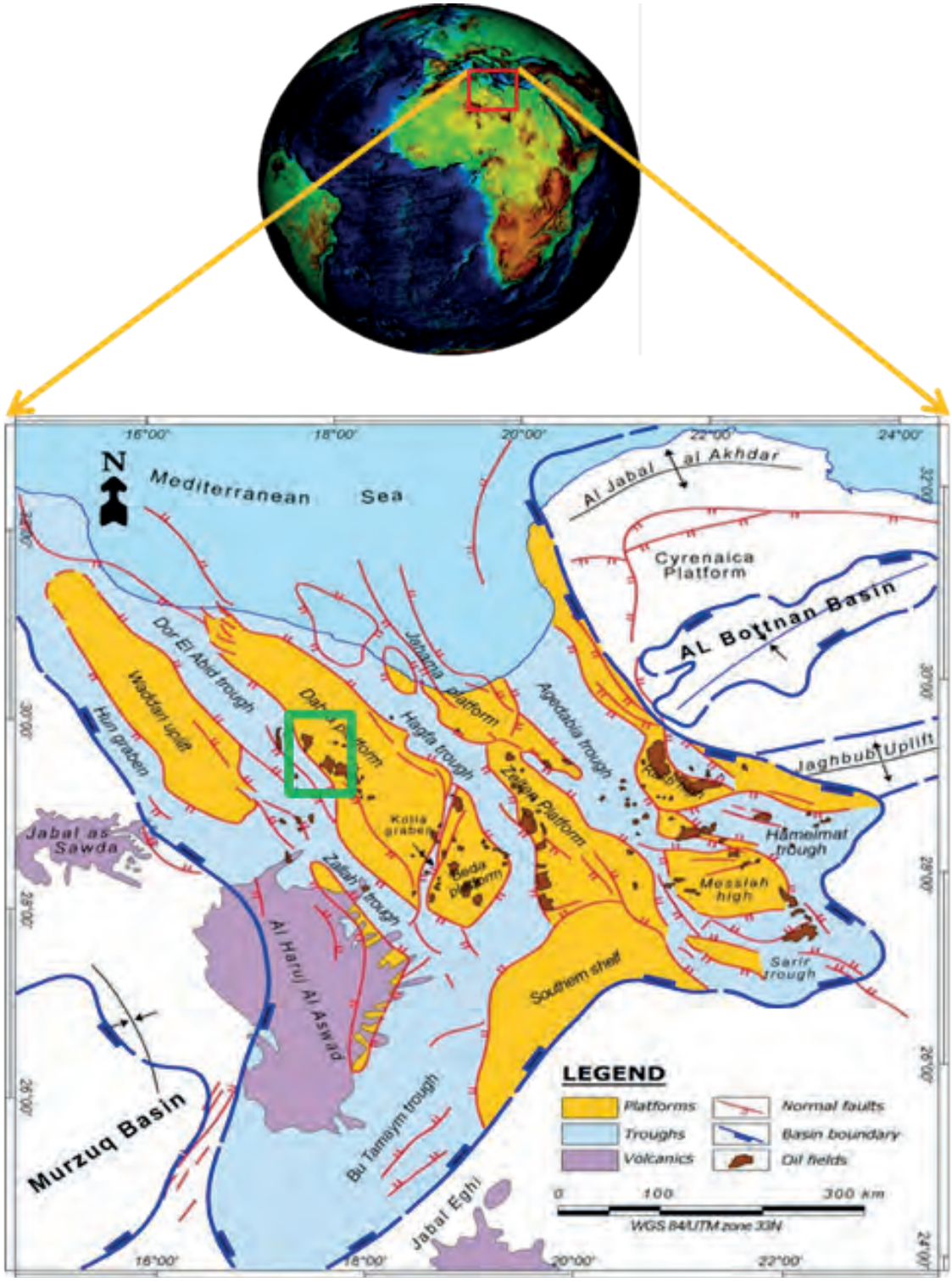

Fig. 1. Location map of the Sirt Basin and its structural elements. The study area in the western Sirt Basin are also shown (After Mouzoghi and Taleb, 1982, and Abadi, 2002).

Sirt Basin and to investigate the effect of these processes on the quality of the Selandian/Thanetian reservoirs. There are few studies of the diagenesis of lower Cenozoic carbonates in North Africa and these Paleocene limestones provide a useful case study of the paragenesis of lime-mud dominated carbonate sediments to lithified limestones and dolomites and the wide range of textures developed.

MATERIALS AND METHODS

This study has been conducted through examination of Well-logs, core samples and thin-

sections (>170) from four wells in the Dahra Field on the Dahra Platform, western Sirt Basin (Fig. 1). The wells are a few kilometres apart and are located several kilometres back from the platform bounding fault. Around 900 feet (275m) of slabbed cores were logged. Thin-sections were stained or half-stained, using the method described by Adams *et al* (1984) adapted from Dickson (1965), and also examined with cathodoluminescence. Microfacies were classified according to Dunham (1962) and Embry and Klovan (1971).

Twenty samples were analysed using secondary electron mode and back-scattered mode of the SEM in the Department of Physics, Durham University and SEM Lab at the Libyan Petroleum Institute in Tripoli. Samples from two wells were analysed for carbon and oxygen stable isotope ratios at the University of Birmingham and fluid inclusions were examined by *Fluid Inclusion Technologies*, Oklahoma, USA. Porosity data were obtained from visual estimates of thin-sections.

GEOLOGICAL SETTING

A change from northward to westward motion of the African Plate in the Late Cretaceous promoted thinning of the cratonic lithosphere on its northern margin (Morgan, 1980, 1983). This was marked by major basin subsidence, reactivation of faults and crustal extension (Gumati and Nairn, 1991; Abdunaser and McCaffrey, 2014). On the northern foreland of the African Plate, subsidence and extensional fault reactivation continued intermittently into the Paleocene and Early Eocene, in response to the relative plate motions of the African, American and Eurasian plates during the opening of the central Atlantic and development of Tethys (Anketell, 1996; Abadi *et al*, 2008). Progressive erosion of younger sediments and subsequent episodes of block faulting resulted in placing the Palaeozoic and Mesozoic reservoirs in a high structural position with respect to thermally-mature Cretaceous source rocks that occupied the deeper portions of the Sirt Basin and its sub-basins.

The stratigraphic succession in the western Sirt Basin (Fig. 2) begins with the Hofra Sandstone of Cambro-Ordovician age overlain unconformably by Upper Cretaceous marine sediments, which, in turn, are succeeded by Cenozoic marine strata (Fig. 2). The Lower Cenozoic sediments are characterized by thick successions of shallow-marine carbonates and deeper-water shales. The latter were generally confined to low-energy zones in elongate basins (troughs) and they also blanketed platforms during phases of flooding and transgression. Carbonates were deposited across platforms and on ramp-type margins into the basins, with their facies controlled by water depth, topography and current-energy level (Gumati, 1982; Abdunaser, 2015).

The Paleocene strata in the Sirt Basin reach a thickness of 650m (~2000ft) on the platforms/horsts, where carbonates dominate, and up to 1000m (~3500ft) in the basinal areas, where the sediments are more muddy. The studied carbonate formations, according to Barr and Weegar (1972) are Dahra, Zelten and Harash. The Dahra, with a thickness of 140m (450ft), the Zelten, 65m (200ft) and the Harash, 45m (150ft). The Khalifa Shale, which separating the Dahra and Zelten formations on the platform is ~45m (150ft) thick.

RESULTS

Sedimentology

The Late Paleocene succession on the Dahra Platform is composed generally of limestone, dolomitic limestone, argillaceous limestone and shale (Fig. 2). There is no evidence from seismic for a shelf break nor from facies analysis for any slope resedimentation; thus, for the most part, the carbonates of the Dahra, Zelten and Harash formations were deposited on a broad flat platform passing to a homoclinal ramp dipping to the west, towards the basin. The platform bounding fault did not create any significant topography between platform and trough, but was responsible for differential subsidence. Macroscopic and microscopic investigations of this succession, which include details of grains, cements, microfabrics, micro-sedimentary structures and diagenetic features, have resulted in the recognition of five main facies and eleven microfacies within the Selandian/Thanetian carbonate succession (Table 1). The macrofacies are: 1) bioclastic foraminiferal packstone/grainstone, 2) foraminiferal bioclastic wackestone-wackestone/packstone, 3) dolomitic lime-mudstone, 4) bioclastic foraminiferal grainstone and 5) nummulitic foraminiferal packstone (Fig. 3). The first four facies have been recognised in the Dahra, Zelten and Harash Formations, whereas, the fifth one, nummulitic foraminiferal packstone only occurs within the Zelten and Harash formations.

The main carbonate grains within the Dahra Formation are rotaliids, miliolids, echinoderms,

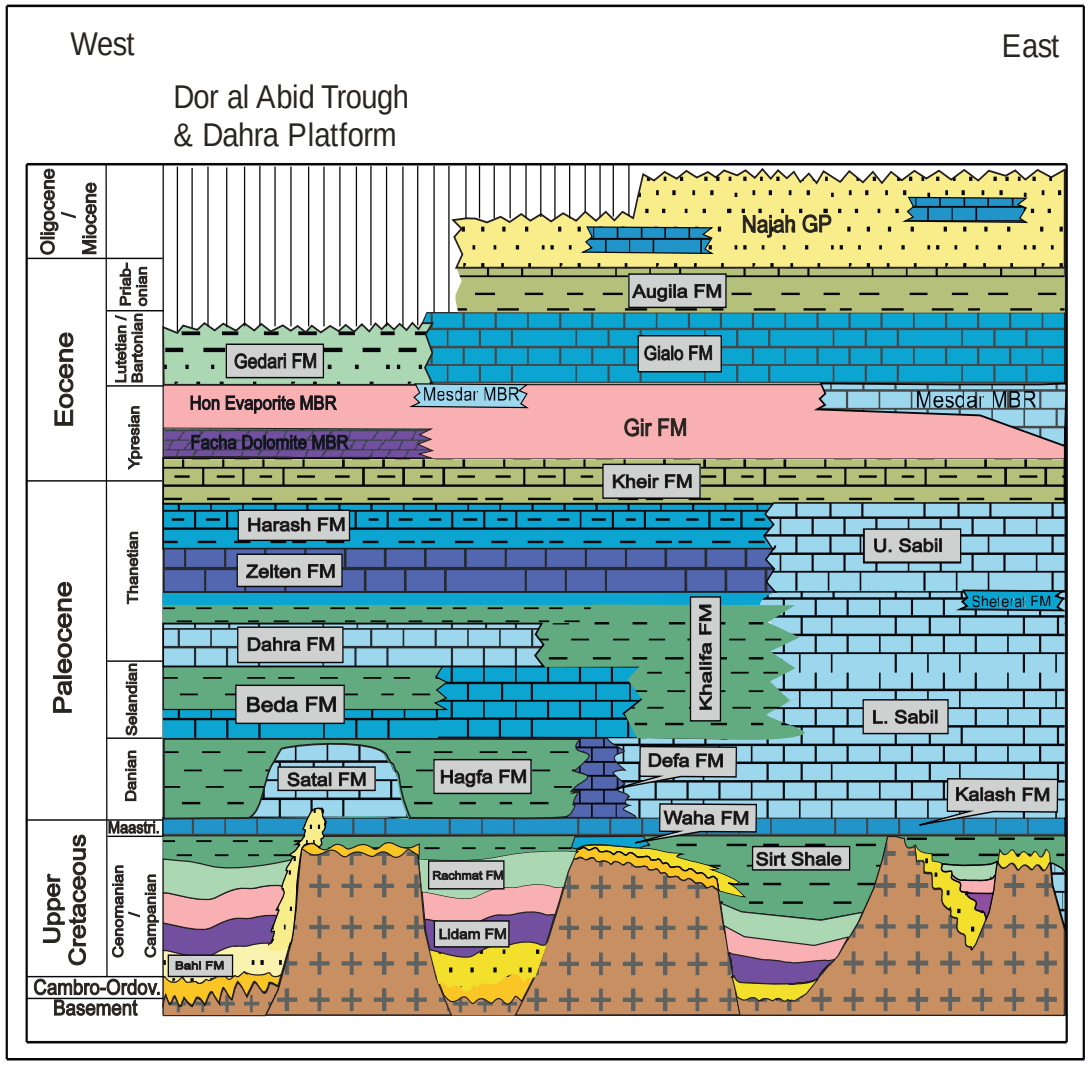

Fig. 2. Generalized stratigraphic and lithologic chart of the northern Sirt Basin. Compiled and modified by the author, 2012 (nomenclature after Barr and Weegar, 1972).

molluscs, ooids, peloids and green algae (Fig. 3A, D & E). Within the Dahra Formation carbonates, shallower to deeper-water facies and microfacies can be recognised, deposited in inner to outer parts of the homoclinal carbonate ramp. The core description, petrographic examination and geophysical logs indicate that there are no drastic changes in the facies and associated microfacies throughout the Dahra Formation; the main variation is in the amount of lime mud originally deposited. The Dahra was probably deposited under similar conditions throughout the east and west Dahra Field on the Dahra Platform, an area encompassing several 100 square kilometres.

The dominant bioclasts within the Zelten and Harash carbonates are benthic foraminifera, molluscan shells, nummulites, *Operculina*, bryozoans and echinoderm fragments (Fig. 3B & F). A similar depositional setting to that of the Dahra Formation was probably re-established in the Zelten and Harash formations across the area, with local occurrences of nummulitic packstone instead of bioclastic grainstone as in the Dahra Formation, and the development of mainly wackestone-packstone.

Surprisingly, except for a generally regressive trend occurring in the late Thanetian, larger-scale transgressive-regressive (T-R) cycles cannot be detected within the Well-logs or cores examined. Thus, there is no correlation with the T-R patterns and eustatic sea-level changes which have been reported for this time-period elsewhere by Miller *et al* (2005) and Ruban *et al* (2010, 2012). The lack of T-R cycles could be a consequence of the data available (poor wireline-log response and/or key horizons missing in core) or a result of the longer-term relative sea-level changes not being recorded within the succession

Table.1. Facies and associated microfacies of the Dahra, Zelten and Harash Formations on the Dahra Platform.

Facies No.	Facies Name	Description	Microfacies	Depositional setting	Remarks
1	Bioclastic foraminiferal packstone-packstone/ grainstone	Light yellowish grey to v. pale orange, locally mottled, m. sorted with abundant benthic forams and shell fragments of different bioclasts. Levels of echinoderms and/or molluscan shells in wells 7 & 8. Locally dolomitic and bioturbated. Slightly argillaceous with sporadic development of stylolites and PDS. Local concentration of iron minerals, particularly in wells 8&10. Overall porosity is fair to good.	Bioclastic foraminiferal packstone/grainstone	Inner ramp (lagoon)	Similar to SMF 10 of Flügel (2004)
			Dolomitic bioturbated bioclastic packstone	Inner ramp (lagoon)	Similar to RMF 7 (SMF 10) of Flügel (2004)
2	Foraminiferal bioclastic wackestone/ packstone	Mainly light grey, locally light yellowish brown or mottled, m. sorted with rotaliids, miliolids, echinoderm fragments and peloids. Planktic forams, red algae, ostracoda and peloids are scattered throughout. Locally dolomitic, bioturbated and slightly argillaceous. Compaction features locally developed, particularly in wells 10 & 8. Iron minerals developed at few intervals in wells 9 & 8. Porosity is poor to fair.	Bioclastic wackstone/ packstone	Inner ramp (lagoon)	Corresponds to RMF 20 or SMF 10 of Flügel (2004)
			Planktic foraminferal wackestone	Mid ramp	Corresponds to RMF 5or SMF 3 of Flügel (2004)
			Dolomitic bioturbated wackestone/packston	Inner ramp (lagoon)	Similar to SMF 10 of Flügel (2004)
3	Dolomitic mudstone	Dolomitic limestone, light yellowish grey to mottled, mod-well sorted with very scattered benthic forams, peloids and gastropod molds. Bored and/ or bioturbated. Locally chalky and/or argillaceous. Porosity is fair to good.	Dolo lime-mudstone	Inner ramp (lagoon)	Corresponds to RMF 19 of Flügel (2004)
4	Bioclastic grainstone	Light grey, light yellowish brown to v. pale orange, m. sorted. Benthic forams, green algae and echinoderms are common with scattered peloids, molluscan shells, intraclasts and bryozoans. Locally dolomitic, bioturbated, and slightly argillaceous. PDS and stylolites. Fe-minerals and syn-sedimentary compaction features in well 10. Porosity is good to very good.	Bioclastic foraminiferal grainstone	Inner to mid ramp Possibly carbonate shoal/ lagoon with an open circulation (back bank)	Corresponds to SMF 10 or 11 of Flügel (2004)
5	Foraminiferal packstone	Light yellowish - light olive grey, hard, poorly-m. sorted, with common nummulites and common to scattered *Assilina*, operculina. bryozoans, echinoderms, molluscan shells and red algae. Slightly argillaceous and bioturbated. Porosity is generally good to v. good.	Nummulitic foraminiferal packstone	Middle ramp, probably foraminiferal bank	Similar to SMF 18 of Flügel (2004)

of the partly-restricted, quite lime-mud dominated, Sirt Basin during the Thanetian. On a global scale, the Late Selandian has been interpreted as a period of relative sea-level stability, and relatively stable climate and tectonics, conditions which persisted into the Early–Middle Thanetian (Ruban *et al*, 2010, 2012). However, higher-frequency metre-scale cycles (2-10 feet in thickness) can be recognised within the Dahra Formation from core, although some are quite subtle (Fig. 4).

Diagenesis Processes and products of the Selandian/Thanetian carbonates

After deposition, the Selandian/Thanetian carbonates in the western Sirt Basin were affected by various diagenetic processes during their burial history, which for the most part was one of continuous increasing overburden. The top of the Paleocene strata on the Dahra platform is currently at a depth of ~1000m and in the adjacent trough at ~1500m. These strata are overlain by the Eocene

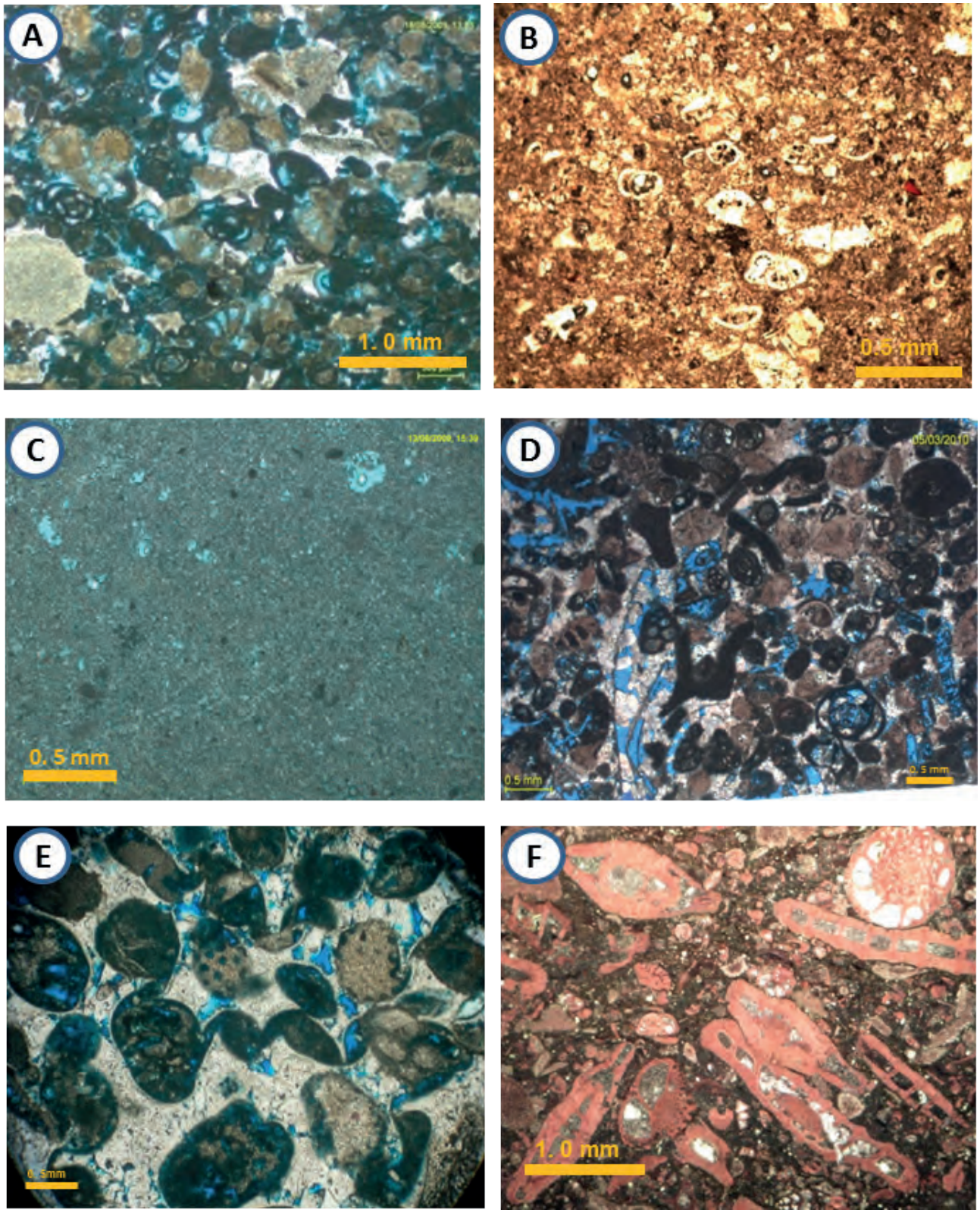

Fig. 3. Macrofacies of the Selandian/Thanetian carbonates in the Dahra Field. A) Bioclastic foraminiferal packstone/grainstone (Dahra Fm, Well no. 8); B) Foraminiferal bioclastic wackestone-wackestone/packstone (Harash Fm, Well no. 9); C) Dolomitic lime-mudstone (Dahra Fm, Well no. 8); D & E) Bioclastic foraminiferal grainstone (Dahra Fm, Well no. 9) and F) Nummulitic foraminiferal packstone (Harash Fm, Well no. 10).

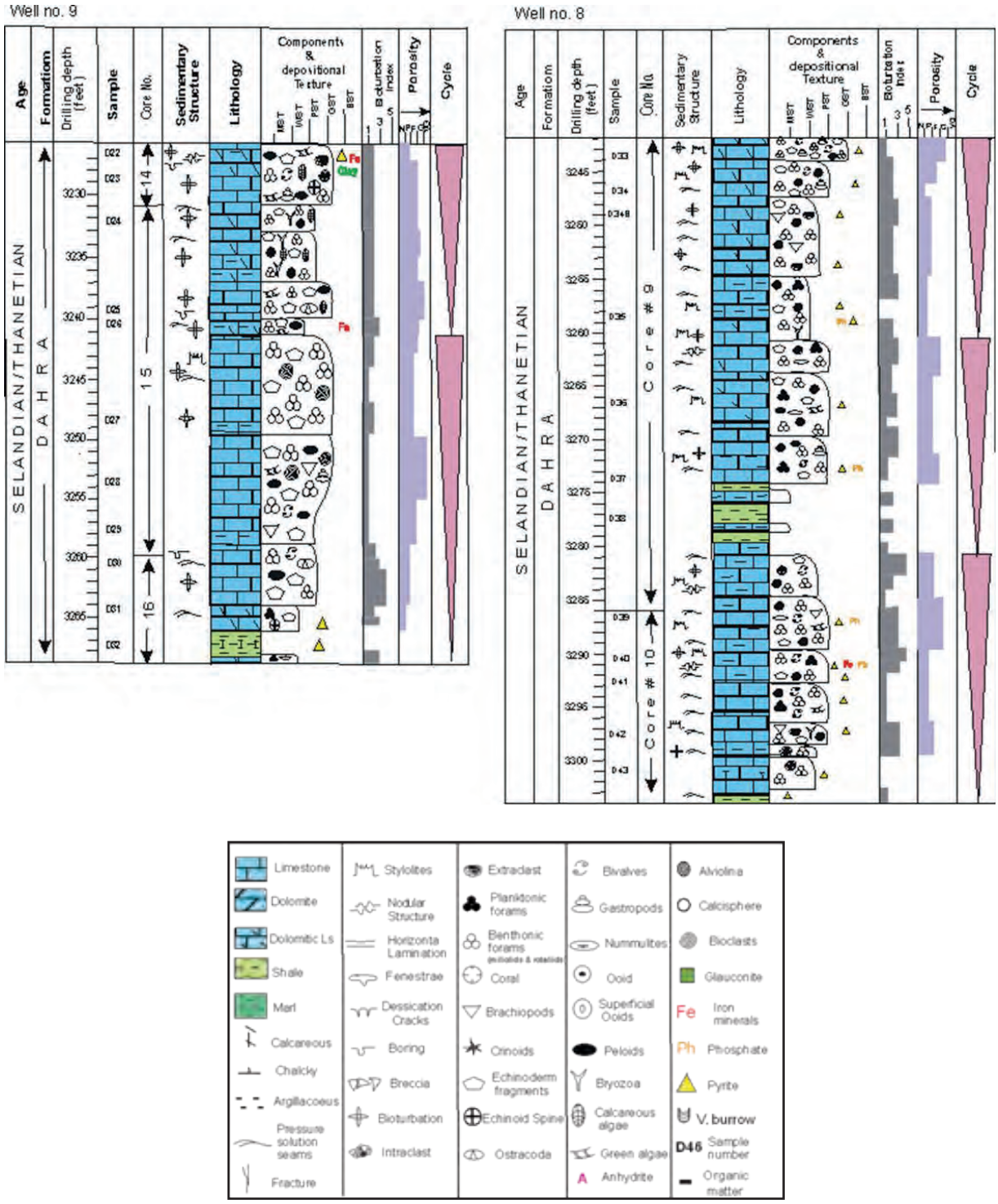

Fig. 4. Sedimentological core logs showing fairly Well-defined carbonate cycles within the Dahra Formation. Well no. 8 and Well no. 9.

Kheir and Gir formations to the present-day surface, although farther east Oligo-Miocene sediments are present too (Fig. 2). The muddy Kheir Formation is a seal to reservoirs in the Harash carbonates. Burial has been interpreted by Van der Meer and Cloetingh (1996) as near constant until the Late-Eocene, after which there was some uplift and erosion. Abadi *et al* (2008) on the other hand, suggested significant uplift and erosion in the Late Eocene-Oligocene, followed by subsidence to the current depth. The geothermal gradient in the Sirt Basin, according to Hallett (2002), averages 25.5ºC/km, and the surface

temperature is about 30ºC (Gumati and Schamel, 1988). Three diagenetic environments have been documented: marine, meteoric and burial; each has its own characteristic features and products.

Marine Diagenesis: Early marine diagenetic processes affecting the Selandian/Thanetian carbonates are represented by local marine cementation and lithification, boring and micritisation of bioclasts. Marine cements are recognised through their first generation occurrence as thin isopachous fringes around grains (Fig.5D). The crystals are acicular to fibrous and reach up to 50 microns in length. In some cases they have a slight pale brown colour relative to later, coarser clear calcite cement. Where there has been mechanical compaction of the limestones during shallow burial, the earlier precipitation of this cement-type is revealed (Fig. 3E). In more muddy facies, local evidence of early lithification is provided by borings which are recorded at several levels in cores of Dahra Platform sediments in the Dahra and Zelten formations. A hardground surface from Well 10 in the Dahra Formation, with borings up to 1mm in diameter, can be observed cutting both grains and substrate (Fig. 5A). The sediment here is a dolomitic packstone with a high concentration of pyrite, glauconite and phosphatic mineral grains.

Hardgrounds are typically developed in areas of slow sedimentation and high current activity at or just below the seafloor (Tucker and Wright, 1990; James and Jones, 2015). The borings are likely produced by polychaete annelids; they are too small to be formed by lithophagid-type bivalves, and they do not have the scalloped margin typical of clinoid borings.

Although micritisation has affected some grains in the Dahra, Zelten and Harash formations, overall it is a fairly rare feature. Repeated boring and filling of holes in a bioclast may result in the formation of a micrite envelope of irregular thickness, and eventually lead to totally micritised grains (peloids) that are smaller than associated skeletal grains. Micritised grains are characterized by an irregular shape, structureless nature, and they mostly range in size from 100 to 300µm (Figs 3D & 5B). Micritisation through microbial alteration is the origin of most peloids, but there are some of probable faecal origin, having a smoother spherical-ovoid shape and smaller size, occurring throughout the succession.

According to Volery *et al* (2009), marine microbial micritisation can be important in generating microporosity within grains. Micritic envelopes formed through endolithic cyanobacteria can be used as a depth criterion, indicating deposition within the photic zone, less than 100-200m (Zeef and Perkins, 1979). Micritisation is an early diagenetic event taking place within the marine phreatic environment, generally in more stagnant, low-energy areas, near or at the sediment/water interface (Longman, 1980). Flügel and Munnecke (2010) noted that microboring endolithic organisms are also found in deeper water. Micritisation is a common feature in Tertiary-Mesozoic shallow-water carbonates (e.g. Madden and Wilson, 2013; Elton *et al*, 2015).

Thus, overall, apart from micritisation, marine diagenetic processes of cementation and lithification are not extensive, occurring only at discrete horizons.

Meteoric Diagenesis: The effects of meteoric diagenesis, manifested in early calcite cementation and grain dissolution as a result of subaerial exposure, can be discerned at several levels within the Paleocene carbonates, but again, these early processes are not widespread.

Calcite cement of meteoric origin occurs in the form of localised to patchy calcite spar crystals to isopachous grain coatings, mainly in the bioclastic foraminiferal packstone-packstone/grainstone and bioclastic foraminiferal grainstone facies. In porous grainy facies, calcite crystals are irregularly distributed between grains and occur within molds resulting from dissolution of bioclasts (Fig. 3D). Rarely a meniscus arrangement of crystals can be discerned, as in occurrences of bioclastic foraminiferal grainstone of Well no. 7 in the Dahra Formation (Fig. 5E). Much porosity is still present (Fig. 3D). Isopachous coatings of bladed to stubby, clear calcite crystals oriented perpendicular to the substrate, mainly occur on the outer, rarely on the inner, walls of both non-skeletal and skeletal grains, particularly foraminifera. The features of this type of cement, notably the non-fibrous bladed fabric, indicate that it is low Mg-calcite of probable meteoric phreatic origin. Meteoric vadose cementation is indicated by meniscus texture, although it can also be formed through microbial activities in other environments (Hillgärtner *et al*, 2001).

Syntaxial overgrowth calcite cement has grown on echinoderm fragments mainly within the grain-dominated facies in the Dahra and Zelten, and less commonly, within the Harash Formation. It rarely occurs in wackestone-packstone facies as a result of the small amount of original pore-space. This cement is commonly a large single crystal developed

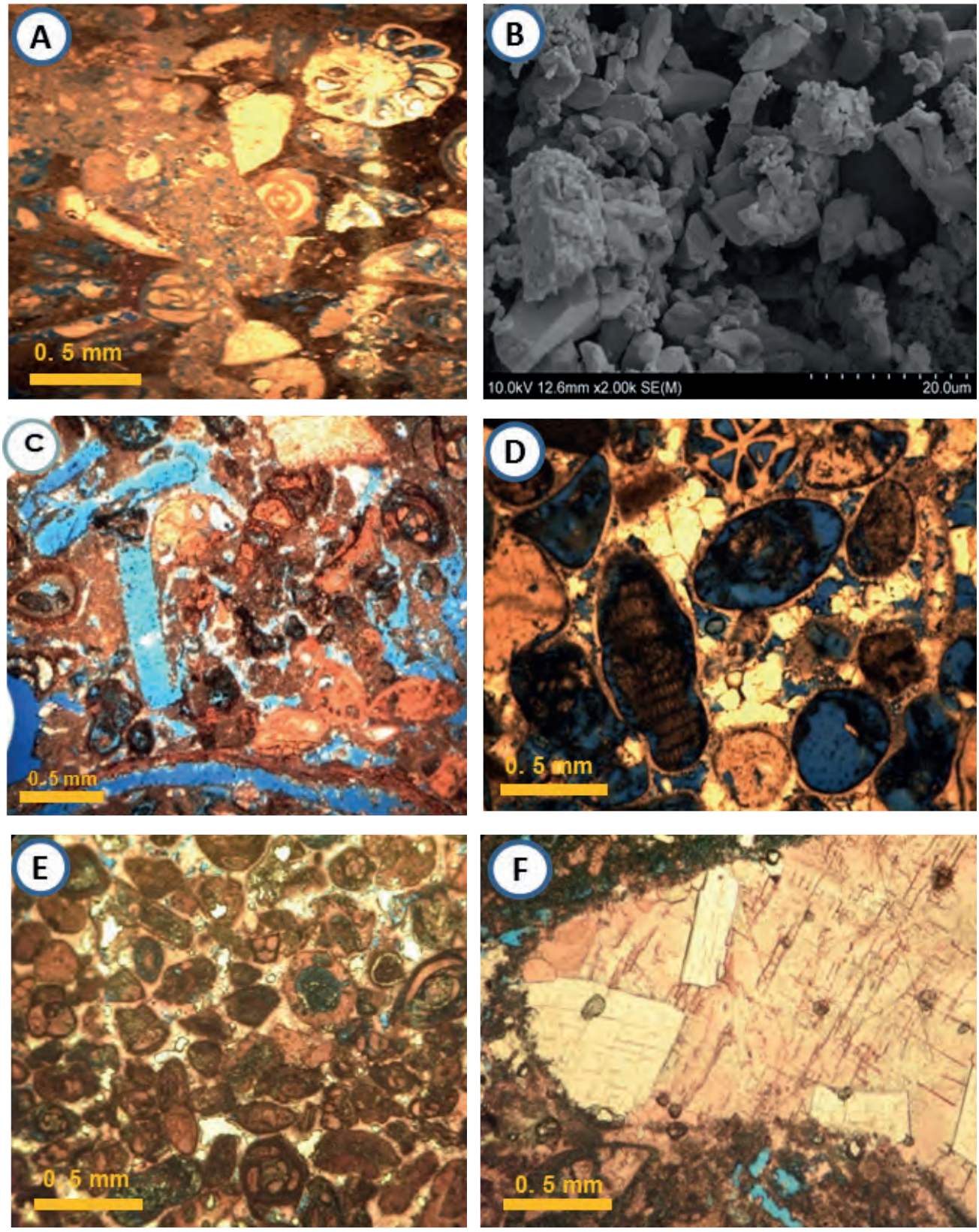

Fig. 5. A) Possible hardground surface, where boring has cut grains and the matrix in the Dahra Fm in Well no.10. B) SEM image of micritized grains in the Dahra Fm in Well no. 9. C) Dissolution (mainly molds) porosity in the Dahra Fm, Well no.10. D) Isopachous calcite cement around bioclasts, followed by equant sparry calcite. Dahra Fm, Well no.10. E) Meniscus vadose cement, Dahra Fm, Well no. 7. F) Very coarse Fe-free calcite cement occludes secondary porosity in bioclastic foraminiferal P-P/G. Zelten Fm, Well no. 7.

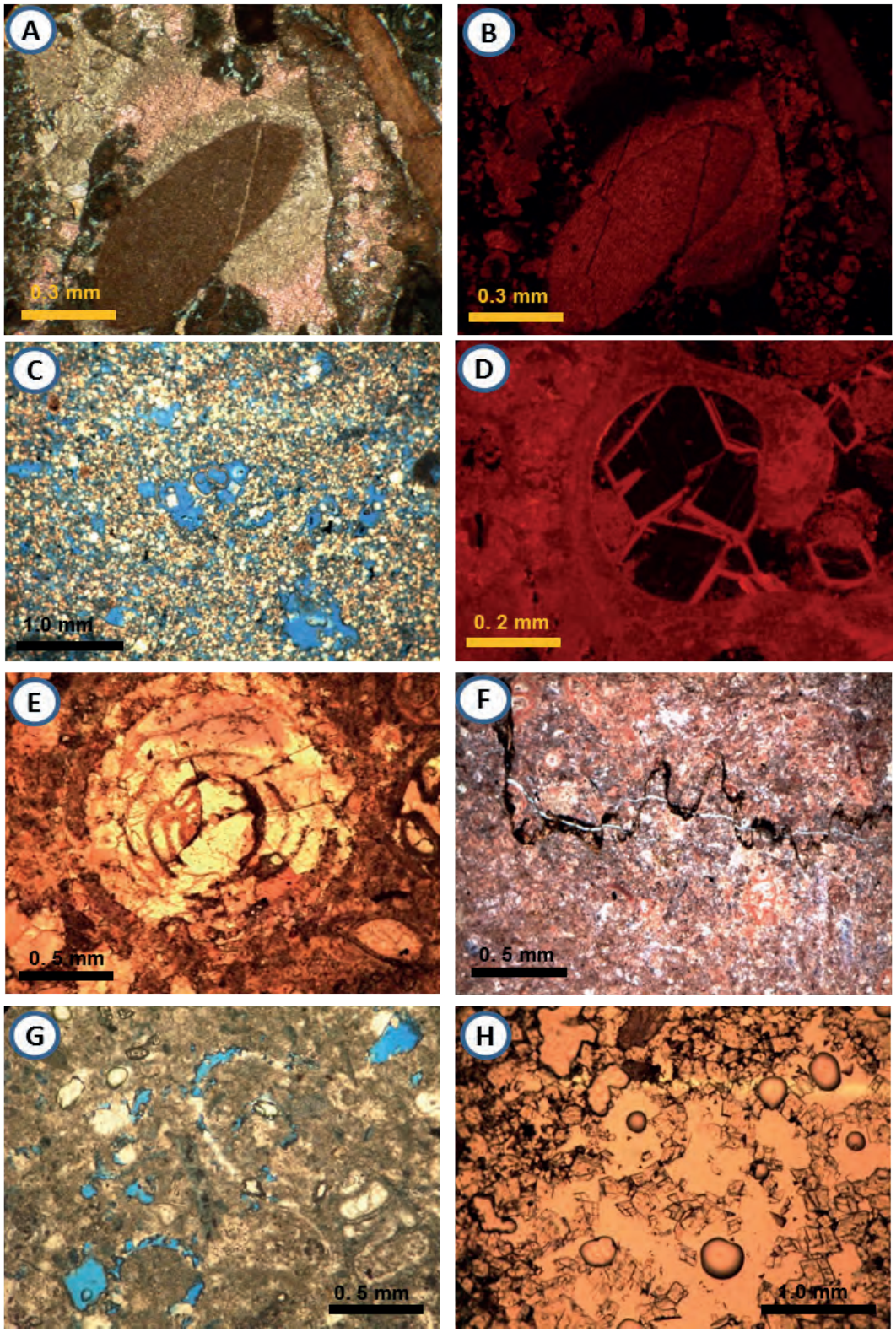

Fig. 6. A & B) Syntaxial rim cement around echinoderm followed by equant calcite cement (pinkish). The CL photo shows that both echinoderm and overgrowth have the same intensity, i.e. light brown to dull luminescence, whereas the equant calcite cement is non-luminescent. Dahra Fm, Well no. 8. C) Very fine-finely crystalline dolomite in dolomitic lime-mudstone facies. Note good intercrystalline and moldic porosity. Dahra Fm, Well no. 8. D) Medium crystalline dolomite filling intragranular porosity. Note the two luminescent characters of dolomite crystals. Dahra Fm, Well no. 9. E) Replacement of Alveolina foraminifera by dolomite and coarse calcite with a retentive fabric, Zelten Fm, Well no.9. F) Microstylolite cuts across matrix, grains and fracture. Dahra Fm, Well no.8. G) Rhomb-shaped pores in bioclastic packstone, Zelten Fm. Well no. 7. H) Extremely porous dolomite resulting from effects of burial dissolution of dolomite and relic limestone. Dahra Fm., Well no. 10.

on echinoid fragments in optical continuity with the grain. Of note is that the overgrowths commonly show two stages of growth, based on staining and cathodoluminescence. The calcite of the inner part of the overgrowth remains unstained whereas, the outer part is pink (Fig. 6A); with cathodoluminescence both echinoderm and the inner part of the growth have the same intensity, i.e. light brown to dull luminescence, whereas, the outer part has no luminescence (Fig. 6B). This pattern could indicate that the inner part has an elevated Mn^{2+} and low Fe^{2+} content, whereas, the outer part has lower Mn^{2+}. This could be the result of the early part being precipitated in a shallow-burial suboxic meteoric setting, and the later part being more of a burial precipitate (Tucker and Wright, 1990).

Post-Compaction Calcite Cementation: Equant sparry calcite cement occurs in most of the grainstone and packstone facies. It may occlude pore space as the second generation cement, following the early marine-meteoric cement, but in many cases there is still porosity present. This sparry calcite consists of clear, equant to elongate crystals, which are locally ferroan.

A drusy mosaic is common, where it occurs as a pore or biomold-filling cement (Fig. 3D). The crystals vary in size from commonly less than 50μm in diameter, locally reaching 200μm at the pore centre. Under cathodoluminescence, the cement crystals are largely non-luminescent to dull (weakly) luminescent, with very thin bright zones towards the outer part of some crystals. This could indicate Fe-rich fluids and the incorporation of Fe^{2+} during the early stage of crystal growth. A change in pore-fluid chemistry to suboxic with the incorporation of manganese into the crystal lattice has probably resulted in the precipitation of the bright outer zones. As stated by Have and Heijnen (1985), the zonation of the carbonate crystals is a reflection of fluctuations in the chemistry of the pore-fluids, but also of changes in the rate of crystal growth. The source of iron may have been clay minerals brought into the environment by continental run-off. A small percentage of terrestrial argillaceous material is finely distributed within the Paleocene carbonates and forms bed-partings and thin layers.

Coarse blocky calcite cement, typically ferroan, with crystals 250-600μm in diameter, in some cases over 1000μm, occurs in the grain-supported facies of the Dahra, Zelten and Harash formations. It usually fills vuggy, moldic, fracture and intergranular porosities and developed as clear, coarse subhedral to euhedral crystals with fairly straight crystal boundaries along with the local occurrence of fluid-inclusions (Figs. 5F & 6E).

Dolomitization: The replacement origin for much of the dolomite is indicated by the presence of ghosts of precursor grains and biomoldic pores, along with the occurrence of completely micritised grains which resisted, to some extent, the dolomitization.

Two types of dolomite are recognised in the Paleocene carbonates: 1) an early fine crystalline dolomite (crystals <20μm**)** which has mainly replaced the matrix in lime-mudstone microfacies of the Dahra Formation (Fig. 3C) ; 2) a medium to coarsely crystalline later dolomite (crystals 100-300μm) occurring as a pore-filling cement mainly in the Dahra Formation and less well developed in the Zelten and Harash formations.

The fine dolomite commonly has a loosely packed subhedral to anhedral crystal mosaic, with a sucrosic texture and good intercrystalline porosity (Fig. 6C). In the Dahra Formation, particularly in Well no. 9, the dolomite is mostly tightly packed and displays hypidiotopic (planar-s) to xenotopic (non-planar) mosaics. It commonly shows fairly good preservation of the original texture and poor intercrystalline porosity. In Wells no. 8 and 10, however, a better preservation of intercrystalline porosity is observed. In Zelten and Harash formations the very finely to medium crystalline dolomite occurs generally as isolated, scattered euhedral to subhedral crystals in the relatively fine-grained matrix of the wackestone/packstone facies.

The local association of this fine dolomite with peritidal features (fenestrae, desiccation cracks, rare evaporite molds, and rootlet structures), particularly in the dolomitic bioturbated wackestone/packstone microfacies, suggests an early diagenetic origin (i.e. eogenetic dolomite). The general lack of evidence for evaporites suggests dolomitization through circulating seawater rather than reflux of hypersaline brines.

Burrowed intervals have commonly been dolomitised preferentially and subjected to a higher intensity of compaction, which in several cases has resulted in the formation of a vaguely bedded fabric, making identification of the original depositional texture (wackestone versus packstone) difficult. Differential dolomitization of the burrowed intervals seems to be controlled by the grain-type (mineralogy) and grain-size of the burrow fill; i.e. many burrows

are completely dolomitised whereas, others are less dolomitic. The finer grain-size of burrow fills as compared with the micritic matrix may be one factor controlling the often observed selective dolomitization of burrow fills (Zenger, 1992). Bio-retexturing can control diagenetic processes because it can selectively increases individual bed permeability where coarse burrow back-filling is dominant. On the other hand, locally it can inhibit early sea-floor cementation by admixing micritic sediment into grain-support fabrics. Feeding, burrowing and irrigation increase solute transport and solid-phase reaction rates, thus leading to rapid carbonate dissolution-replacement (Green and Aller, 1992; Gingas *et al*, 2004; Rameil, 2008).

The medium to coarsely crystalline dolomite (100-300μm) usually occurs as a pore-lining and/or pore-filling cement and thus, contributes to reducing, and more commonly occluding, the intergranular, intragranular, moldic, vuggy and fracture porosities. It is characterised by single, usually non-ferroan, euhedral to subhedral crystals, locally with curved crystal faces; it may display some Cl-zonation (Fig. 6D).

In the Zelten/Harash formations coarse dolomite is commonly associated with the late, coarse, Fe-free calcite cement and together they plug remaining porosity (Fig. 5F). The dolomite rhombs are mostly weakly to non-luminescent, with a thin outer zone of bright orange colour (Fig. 6D). This pattern is probably reflecting a change in pore-water chemistry from iron-rich to iron-poor/Mn-rich, in response to a change of redox conditions (Tucker and Wright, 1990). It has been suggested that the amount of manganese necessary to induce bright luminescence in carbonates ranges from 80 to 100ppm (Machel and Burton, 1991). Some of these larger dolomites show undulose extinction, a strong, slightly curved cleavage and so are of the saddle/ baroque type.

Authigenic Clay Minerals: Apart from clay within more argillaceous limestone facies and thin clay layers and beds, clay minerals of probable authigenic origin have developed within the limestones, notably within wackestone-packstone intervals in the Dahra Formation. Minerals recognised on the basis of good-crystal form under SEM and EDS analysis include kaolinite, chlorite, illite and probably mixed-layer illite/smectite. They have been precipitated within intergranular cavities, and between calcite spar crystals (Fig. 7). In some cases the clay minerals have occluded the porosity.

Authigenic clay minerals are relatively rare in limestones compared to sandstones, although they do occur in fractures and vugs and along stylolites (e.g. El Hefnawi *et al*, 2010). As in sandstones, the clays can have a significant effect on porosity and permeability.

Compaction and Fracturing: Macroscopic and microscopic examination of the rocks under investigation revealed that they have been subjected locally to considerable compaction (physical and chemical) and to less significant fracturing.

The effects of mechanical compaction are found most commonly in grains that were affected by boring, leaching, or other grain-weakening processes during marine or meteoric diagenesis. Mechanical compaction in which some bioclasts, in particular foraminiferal tests, were crushed and/ or flattened were observed in the Dahra, Zelten and Harash formations. Closer packing and deformation features are more common in the mud-supported facies. Fracturing of grains (mainly bivalve shells) and substrate is widely developed in the packstone/ grainstone facies of the Dahra Formation. Many superficial ooids and coated grains show breakage and cracking along the lamellae and as a result the cortical layer or an early isopachous cement coating has spalled off, and intragranular secondary porosity has been produced (Fig. 5D). Mechanical compaction, which was probably accompanied by, or occurred just after, partial leaching of the grains, has produced deformed ooids. Some show the 'elephant-parade' (or 'trunk-to-tail') fabric of Folk and Lynch (2001), particularly in the middle interval of the Dahra Formation (Fig. 3E). Later equant calcite cement was precipitated within the cavities developed in the ooids and between compacted grains, although in many cases a fair amount of porosity has remained unfilled. Most of these mechanical compaction features would have occurred at shallow burial depths where the Upper Paleocene carbonates were semi-indurated by the early cement crusts of marine or meteoric origin. Indeed, the presence of the cement fringes around the grains, locally spalled off, alongside the patchy leaching of the grains themselves, suggests some mineralogical difference between the two (grains and cement), and leaching through meteoric water influx. The local patchy sparry calcite cement occurring within and between the ooids could be precipitated from meteoric water too, post-compaction, in the shallow-burial realm. Tucker (Pers. Commu.)

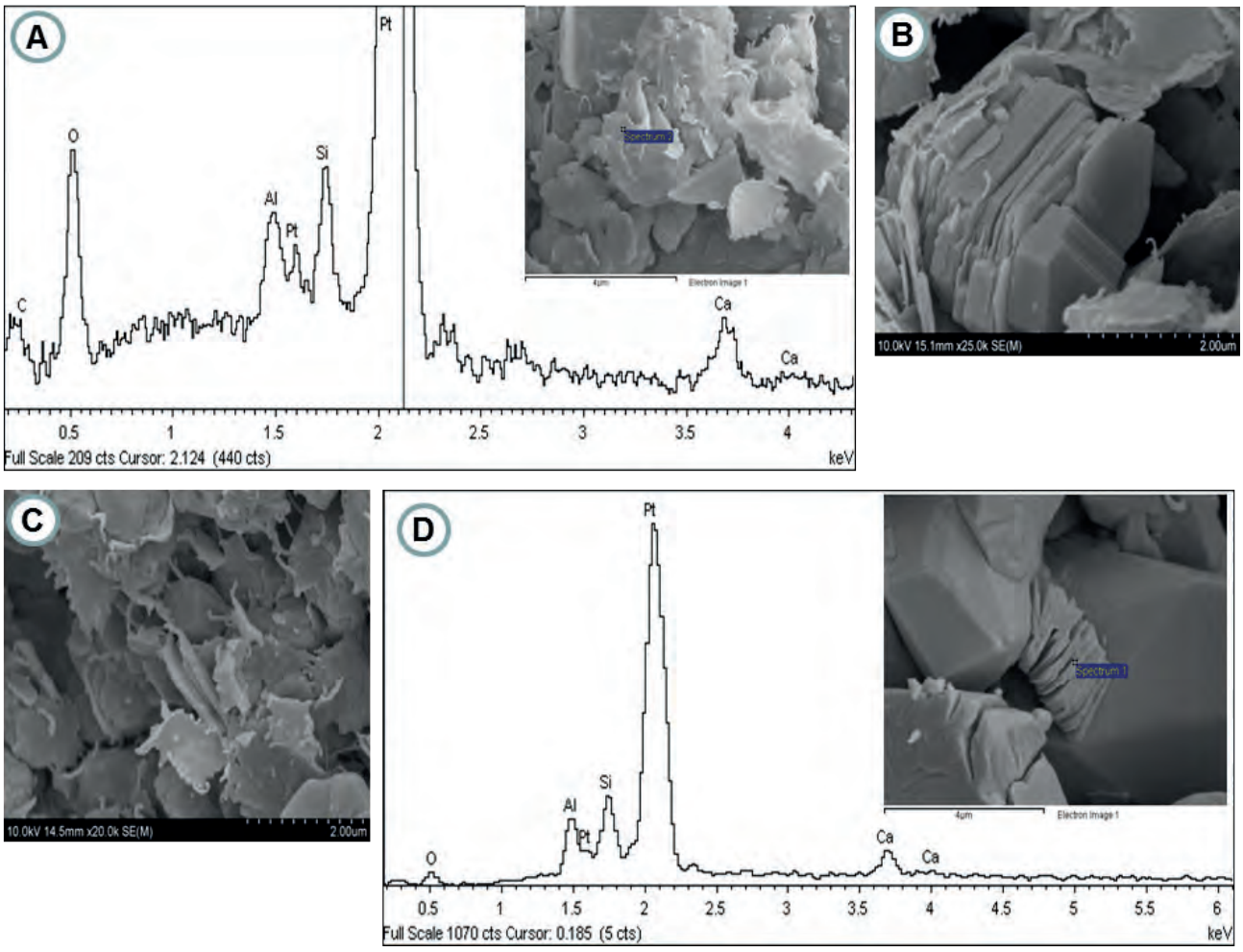

Fig. 7. SEM analysis of the clay minerals identified within the Paleocene succession. A: Smectite mineral between micrite crystals. The chemical composition of this smectite is shown in the EDS spectra. B: Kaolinite (book sheets) plugging intercrystalline porosity in bioclastic wackestone/packstone facies. (A&B) from the Dahra Fm, Well no. 9. C & D: Illite and kaolinite minerals from the Dahra Formation in Well no. 8 at depths of 3185 ft (970 m), and 3119 ft (950 m), respectively.

has noted mechanical compaction in Pleistocene aeolianites, which had less than 100m of overburden.

Networks of microfractures that interconnect different types of porosity have been observed in most of the Paleocene carbonate facies. They have been recorded chiefly in the Dahra and Harash formations, with fewer in the Zelten Formation. They are commonly open and in some cases crossed by stylolites (Fig. 6F). Stronger fractures and minor faults have been encountered in core, and a possible strike-slip fault with vague striations was observed in the lower interval of the Harash Formation in Well no. 9. Two intervals, ~ 1 metre thick, of fractured limestone were noted in the Dahra Formation at Wells no. 8 and 10.

Dissolution seams occur at many intervals in the studied rocks, particularly in the argillaceous limestone facies. They display fairly smooth, undulose seams of insoluble residue and usually pass between and around grains. Dissolution seams tend to be common in more argillaceous limestones, and develop preferentially along the clay layers or at the junctions of clay-rich and clay-poor limestones. Sutured contacts between carbonate grains have resulted in the formation of stylo-nodular structure or stylo-breccia fabric (cf. Logan and Semeniuk, 1976) at several intervals, especially in the Dahra Formation. In terms of petroleum reservoir quality, the pressure dissolution processes lead to a strong reduction in bulk rock-volume with a resultant loss in porosity caused by the occlusion of pores by late diagenetic cement (Wong and Oldershaw, 1981; Swati *et al*, 2014).

Stylolitization normally contributes to bulk volume reduction, resulting in a marked drop in the original thickness of carbonate units (Flügel and Munnecke, 2010). A variety of stylolite types is developed including large amplitude, small

amplitude and swarm types, and they usually cross-cut grains, matrix and cements. In some cases they are associated with fractures (Fig. 6F). They are commonly filled by insoluble residue (probably clay), which was derived from limestone dissolution, and pyrite. Locally, particularly in the Dahra, bitumen and finely crystalline dolomite are also present with the insoluble residue. Stylolites can be significant in the creation of permeability barriers within reservoir facies (e.g. Ebnor *et al*., 2010; Rustichelli *et al*, 2015).

In addition, there are other minor diagenetic events recognized in the Late Paleocene succession, which include precipitation of authigenic pyrite, glauconite, hematite, phosphate and anhydrite.

Burial Dissolution: Evidence of dissolution, both early and late, is widespread in the Paleocene carbonates, with at least two major phases of dissolution: one near-surface and the other later, during burial. The first phase caused the dissolution of the original aragonitic, and probably high Mg-calcite grains together with some matrix. This has resulted in the formation of moldic and vuggy secondary porosity which is present in most of the defined facies of the Dahra, Zelten and Harash formations, but to different degrees (Fig. 5C, D). Much of this porosity has subsequently been occluded, partly or completely, by equant non-ferroan, locally ferroan, calcite or dolomite cements.

The relatively early phase of dissolution probably occurred in the upper part of the meteoric phreatic environment, where the meteoric waters are strongly undersaturated with respect to the metastable carbonate species. Meteoric diagenesis starts with the loss of magnesium from high-Mg calcite followed by the gradual disappearance of aragonite and the replacement of aragonite by calcite (Flügel and Munnecke, 2010). Although dissolution is a major process in near-surface, meteoric, diagenetic environments, it can also take place on the sea-floor and during deep burial (Tucker and Wright, 1990).

The second phase of dissolution has caused the partial to total dissolution of the medium to coarsely crystalline void-filling dolomites. As a result, moldic porosity or dedolomite porosity has been developed, notably in the Dahra and Zelten formations (Fig. 6G, H). This type of porosity has probably been formed by leaching of dolomite crystals at intermediate to deep burial depths, probably through the presence of strong acidic formation waters, rather than early during subaerial exposure and dissolution by karst waters (Nader *et al*, 2008). The dissolution of carbonates in a deep burial setting is attributed to the development of pore waters with high pCO_2 formed during the thermal decarboxylation of organic matter or to sulphate reduction (Mazzulo and Harris, 1992). However, there has been much discussion over the significance of burial dissolution in recent years, with the consensus being that it is a significant process and may lead to much porosity creation (see Ehrenberger *et al*, 2012; Wright and Harris 2013; Van Berk *et al*, 2015; Barnett et al. 2015; Chandra *et al*, 2015).

Isotope Geochemistry of the Selandian/Thanetian Carbonates

In general, the original carbon isotopic composition of a marine carbonate sediment is more resistant to diagenetic alteration (unless there is significant organic matter present undergoing decomposition), compared to its original oxygen isotopic signature. The latter is susceptible to change resulting from meteoric diagenesis and changes in pore-fluid isotopic composition, and increased temperature through burial, leading to cementation-neomorphism and generally more negative $\delta^{18}O$ values of carbonate. In view of the generally fine grain-size of the Paleocene carbonates, including the grainstones, whole rock samples were analysed although the least grainy samples were chosen where possible, since the objective was to determine the original variation, stratigraphy and the degree of diagenetic alteration.

Carbon Isotope Stratigraphy: The Dahra Formation shows a quite narrow range in $\delta^{13}C$ values, in Well no. 8, between +1.0‰ and +3.5‰ (except for one likely 'rogue' data point of -1.8‰) and an average value of +2.16‰. The $\delta^{13}C$ values in the Dahra in Well no. 9 range between +1.2‰ and +3.1‰, with an average of +2.44‰ (Figs. 8 &9).

Plotted stratigraphically, the carbon isotope values of the two Wells in the Dahra Formation show no significant change up through the section (apart from the 'rogue' point near the top of Well no. 8 (Fig. 8). This suggests that $\delta^{13}C$ seawater did not change significantly through the period of deposition, and that there was little diagenetic alteration of the $\delta^{13}C$ values, as through the effects of organic matter decomposition in a soil zone during subaerial exposure or during burial.

The carbon isotope values of the Zelten and Harash formations in the east and west Dahra fields are quite similar and confined to a narrow range between +2.22‰ to +3.89‰. The average $\delta^{13}C$ value

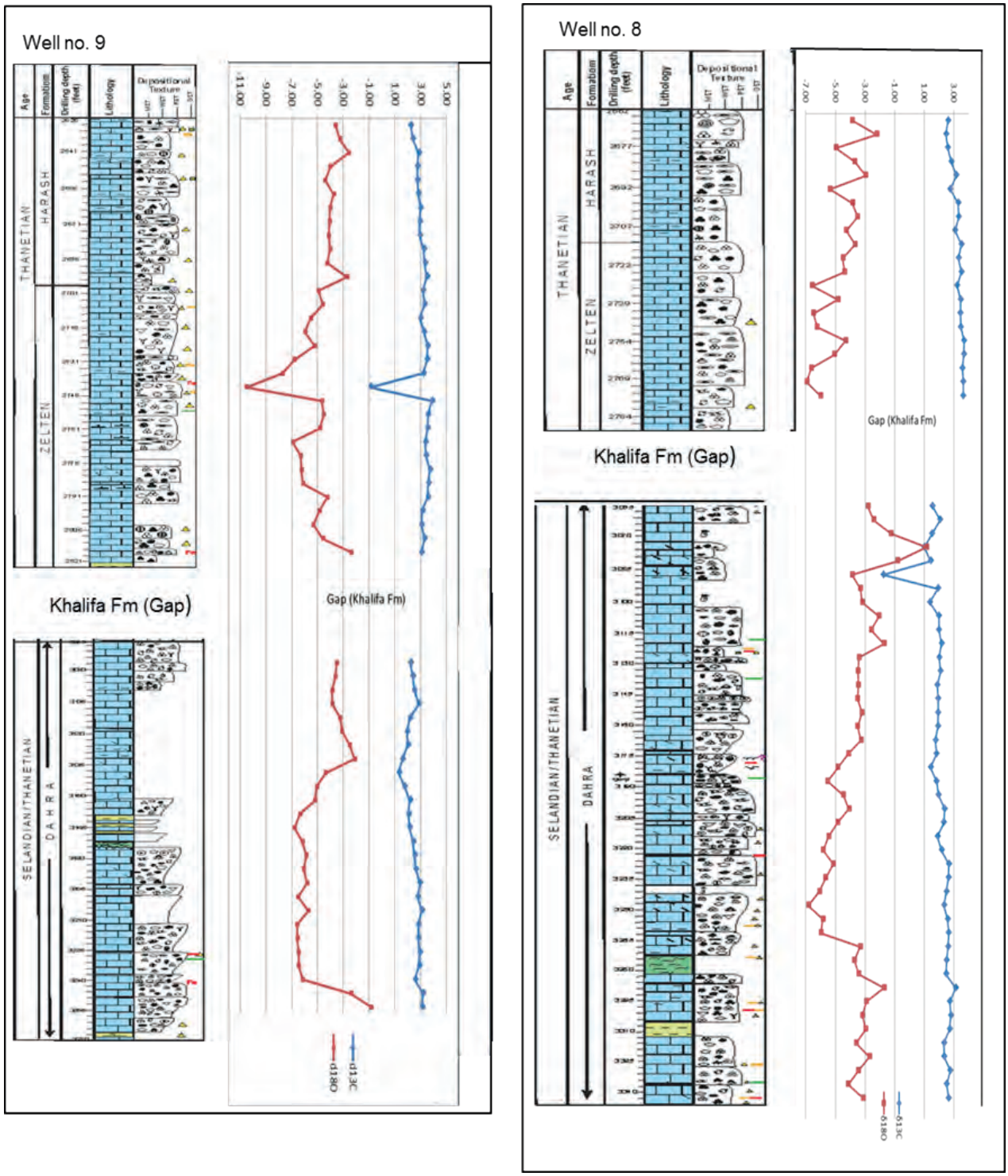

Fig. 8. Carbon versus oxygen isotopes of the studied Selandian/Thanetian succession (Dahra, Zelten and Harash Formations in Wells no. 8 & 9 on the Dahra Platform.

for Well no. 8 is 3.23‰ and for Well no. 9 is 3.17‰. Compared to the Dahra Formation, these averages are a little more positive. Plotted stratigraphically, the carbon isotope stratigraphy for the Zelten-Harash strata shows little change up-section, in both Wells 8 and 9, except for one likely rogue point of -1 ‰ in Well 9. Again this suggests a stable carbon isotope composition of seawater, in this case through much of Thanetian time, with no significant diagenetic alteration.

During the Upper Paleocene the $\delta^{13}C$ signature of marine carbonate is generally between +1 and +2, before the sharp excursion to less positive values of +1 to 0 ‰ or low negative values at the Paleocene-

Eocene Thermal Maximum (PETM) (e.g. Koch *et al*, 2003; Zachos *et al*, 2006). There is also a sharp negative excursion in $\delta^{13}C$ within the late Selandian, which has been referred to as the Mid-Paleocene Biotic Event (MPBE, Pujalte *et al*, 2003; Bernaola *et al*, 2009). The carbon isotope stratigraphy for the Upper Paleocene on the Dahra Platform in the Sirt Basin presented here (Fig. 8) does not show any clear excursions. The two negative data-points, one in Well 9 and one in Well 8, are not present in both wells at the same horizon, hence they are interpreted as 'rogue' values with no stratigraphic significance. It would thus appear that the studied intervals of the Dahra and Harash are above the MPBE and below the PETM.

Oxygen Isotope Stratigraphy: The oxygen isotope data in the Dahra Formation, by way of contrast to $\delta^{13}C$, are much more scattered: between -6.8‰ and +1.1‰ in Well no. 8 (average -3.63‰), and between -6.7‰ and-0.8‰ in Well no. 9 (average -4.81‰) (Fig. 9). Plotted stratigraphically, the data show several pronounced shifts (Fig. 8). In Well no. 9 there is a trend from low negative (-0.8‰, depth 3268ft/995m) to more negative values (~-6.1‰, depth 3260ft/992m), and then a return to low negative values towards the top of the formation. In Well no. 8, there is a somewhat similar pattern, although with a longer section towards the base of low negative values (depths 3334-3259ft/1015-9933m). In the uppermost part of the Dahra Formation in Well no. 8, there is a positive excursion with $\delta^{18}O$ increasing from -3.79‰ to +1.15‰, and then reducing to -1‰. With the $\delta^{13}C$ in Well no. 8 at this level, apart from the one 'rogue' negative value, there is no significant change in this part of the section. This uppermost part of the Dahra is occupied by dolomitic, slightly bioturbated wackestone facies that is characterised by the development of desiccation cracks and fenestrae, indicating subaerial exposure. The positive $\delta^{18}O$ values coinciding with the occurrence of dolomite could indicate a near-surface precipitate from seawater (Tucker & Wright 1990). The negative values $\delta^{18}O$ values elsewhere in the core indicate meteoric or burial processes.

The oxygen isotope values in the Zelten and Harash formations range from -10.49‰ to -2.21‰, with an average of -4.60‰ in Well no. 8 and -4.77‰ in Well no. 9 (Figs. 8, 9). Plotted stratigraphically, the $\delta^{18}O$ data in Well no. 8 show a 'zig-zag' pattern but there is a long-term trend from more negative (-6‰) to less negative (-3 ‰) over the core thickness of some 40 metres. In Well no. 9, there are again small-scale variations in $\delta^{18}O$, and one much more negative data-point (at -10.5‰ at 2742ft/835m), but overall there is a weak trend from low negative (-3‰) to more negative (-7‰) in the upper Zelten, and then back to less negative (-3‰) from the upper Zelten through to the top of the core in the Harash.

The $\delta^{18}O$ values of marine carbonate in the upper Paleocene are 0 to -2‰, depending on palaeolatitude and facies (Koch *et al*, 2003; Zachos *et al*, 2006). The $\delta^{18}O$ values shown by the Dahra, Zelten and Harash formations are mostly much more negative than these, averaging-4.3‰, apart from the upper part of the Dahra Formation in Well no. 8. The samples with $\delta^{18}O$ more negative than 3 are likely to have been altered by diagenetic processes. However, the data plotted stratigraphically are not completely random; there are long-term trends in the $\delta^{18}O$ data through the succession, which are interpreted here as reflecting original fluctuations in environmental conditions.

Following the MPBE and up to the PETM a long-term phase of warming has been recognised before the extreme thermal maximum of the PETM itself, which is represented by a sharp negative $\delta^{18}O$ excursion (Koch *et al*, 2003; Zachos *et al*, 2006). Climatic warming through the Selandian-Thanetian would be recorded in the $\delta^{18}O$ stratigraphic record as a long-term trend towards more negative values, from around 0 to -1 ‰ to closer to -2‰ or -3‰ as temperature increased. There is little indication of a long-term negative trend in the Libyan $\delta^{18}O$ data (Fig. 9); if anything the long-term trends are the other way, towards less negative values, as in the Harash Formation in both Wells no. 8 and 9, and in the Dahra in Well no. 8.

Overall then, it would, appear that the oxygen isotope data do not preserve the expected patterns reported from other Paleocene sections. The values themselves are more negative than most original values expected for the Paleocene; this would most likely be the result of diagenesis, through near-surface meteoric fluids with their typically more negative $\delta^{18}O$ composition compared to seawater and/or precipitation of cements during burial, with the higher temperatures there.

Fluid Inclusion Results

Several representative samples of coarse calcite crystals were examined for their fluid inclusions. The inclusions are generally absent to rare, but there are some crystals where they are relatively common.

Inclusions are normally 3-6µm in diameter and are filled with oil or water. The inclusions fluoresce with colours ranging from yellow to white, with some being blue (Figs. 10, 11). Sample no. 49, from the Dahra Formation at a depth of 3229ft (985m) in Well no. 8, shows several white fluorescent inclusions within coarse late calcite in a porous dolomitic grainstone (Fig. 10 and Table 2). Sample no. 46 from the Dahra Formation in Well no. 9 at a depth of 3216 ft (980m) contains several to many inclusions with a blue fluorescent colour in calcite cement within a porous bioturbated grainstone.

In the Zelten Formation, Well no. 8, sample no. 21 (depth 2788ft/850m), a high oil saturation is detected suggesting an oil column or palaeo-column. Calcite crystals contain a high visual abundance of yellow fluorescent inclusions in a non-porous wackestone/packstone (Fig. 11 and Table 2). In the Harash Formation in Well no. 9, sample no. 13 (2698 ft/825 m), on the other hand, rare to several white fluorescent inclusions in calcite occur in a non-porous packstone.

Measurements taken on inclusions containing hydrocarbon from the Dahra Formation show that the

Table 2. Fluid inclusion results of sample no. 49, the Dahra Fm, Well no.8 (A); Sample no. 46, the Dahra Fm, Well no. 9 (B); Sample no. 21, Zelten Fm, Well no.8 (C), and sample no. 13, the Harash Fm, Well no. 9 (D).

Well no. 8 – 2788 (Z)						
Population	**Fluor Color**	**Th hc (°C)**	**API hc (°)**	**Th aq (°C)**	**Tm aq (°C)**	**Sal (wt%)**
pr/sec; cc	wt	63 (1)				
pr/sec; cc	wt	60 (1)				

Well no.9 -3216 (D)						
Population	**Fluor Color**	**Th hc (°C)**	**API hc (°)**	**Th aq (°C)**	**Tm aq (°C)**	**Sal (wt%)**
pr/sec; cc	bl	59 (2)				
pr/sec; cc	bl	54 (1)				
pr/sec; cc	bl	67 (1)				

Well no. 8 – 2788 (Z)						
Population	**Fluor Color**	**Th hc (°C)**	**API hc (°)**	**Th aq (°C)**	**Tm aq (°C)**	**Sal (wt%)**
pr/sec; cc	wt	57 (1)				
pr?/sec; cc	wt	48 (1)				
pr?/sec?; cc				59 (1)	-10.5	14.5

Well no. 9 – 2698 (H)						
Population	**Fluor Color**	**Th hc (°C)**	**API hc (°)**	**Th aq (°C)**	**Tm aq (°C)**	**Sal (wt%)**
pr/sec; cc	wt	60 (1)		90 (1)	-4.1	6.6
pr/sec; cc				67 (1)	N/A	N/A
pr; cc				70 (1)	-21.2	23.1

Legend

Fluorescence Color: based on illumination with Nikon UV-2A filter
Th hc: homogenization temperature of petroleum inclusions
API hc: measured or estimated API gravity of petroleum inclusions

Th aq: homogenization temperature of aqueous inclusions
Tm aq: final melting temperature of aqueous inclusions
mixed: inclusion contains aqueous fluid and petroleum
metastable: final Tm above 0 C precludes accurate salinity

NOTE: data on same line indicate coexisting aq and pet

Sal (wt%): salinity computed from NaCl-H2O system
Capital Letter: population or area

Number in Parentheses: number of inclusions measured
N/A: could not be determined
S?: high Th from deformation of inclusion cavity
pr: primary
sec: secondary
psec: pseudo-secondary

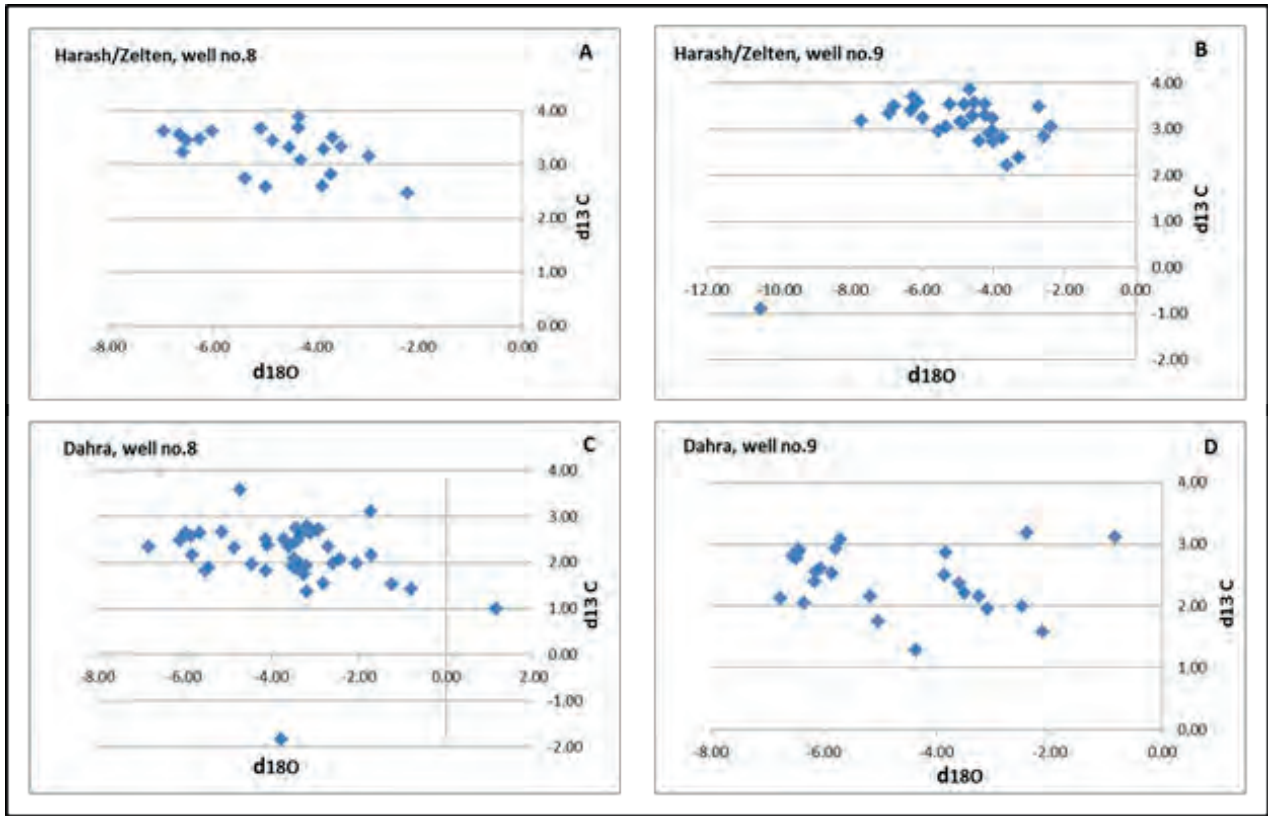

Fig. 9. Oxygen and carbon isotopes for the Zelten and Harash Formations (A & B) and Dahra Formation (C & D) in Well no. 8 and 9. Dahra Field on the Dahra Platform.

homogenisation temperature ranges between 48 and 67^{0}C. With aqueous inclusions, the homogenisation temperature varies from 59 to 90^{0}C (Table 2). The homogenisation temperature of both petroleum and aqueous inclusions against frequency is shown in (Fig. 12).

The homogenisation temperature from hydrocarbon inclusions in the Zelten Formation is between 48 and 57^{0}C, and in the Harash Formation it is 60^{0}C. The homogenisation temperature of aqueous inclusions in the Zelten Formation is 59^{0}C, and in the Harash Formation it ranges between 67 and 90^{0}C (Table 2). The homogenisation temperature of the aqueous inclusions is higher than that of the petroleum inclusions in the Zelten Formation, and is much higher in the Harash Formation. This could suggest two phases of calcite precipitation, an earlier, shallow burial one coinciding with some hydrocarbon generation, and another later, somewhat deeper phase of calcite precipitation.

The maximum temperatures of homogenisation, reaching 90^{o}C, indicate that burial depths of cementation were the order of 2000 metres (geothermal gradient 25^o/km). With the Paleocene carbonates at a depth of 700-1500m, this supports the interpretation of Abadi *et al* (2008) of significant uplift in the Oligo-Miocene.

DISCUSSION

Paragenesis

The relative timing of diagenetic features in the Selandian/Thanetian carbonates has been considered on the basis of petrographic observations and cross-cutting relationships between diagenetic fabrics. A paragenesis for these carbonates is presented in (Fig. 13).

Evidence of early marine diagenesis is recorded throughout all 3 formations and is represented by local acicular fibrous cement coatings of grains, lithified sediment forming hardgrounds penetrated by borings, microbial micritisation and formation of micritic envelopes. The early rim cement has preserved some primary intergranular porosity in certain levels of the Dahra Formation. On the whole, the degree of marine cementation is minor.

Dissolution of grains of metastable mineralogy, and precipitation of calcite cement with a meniscus

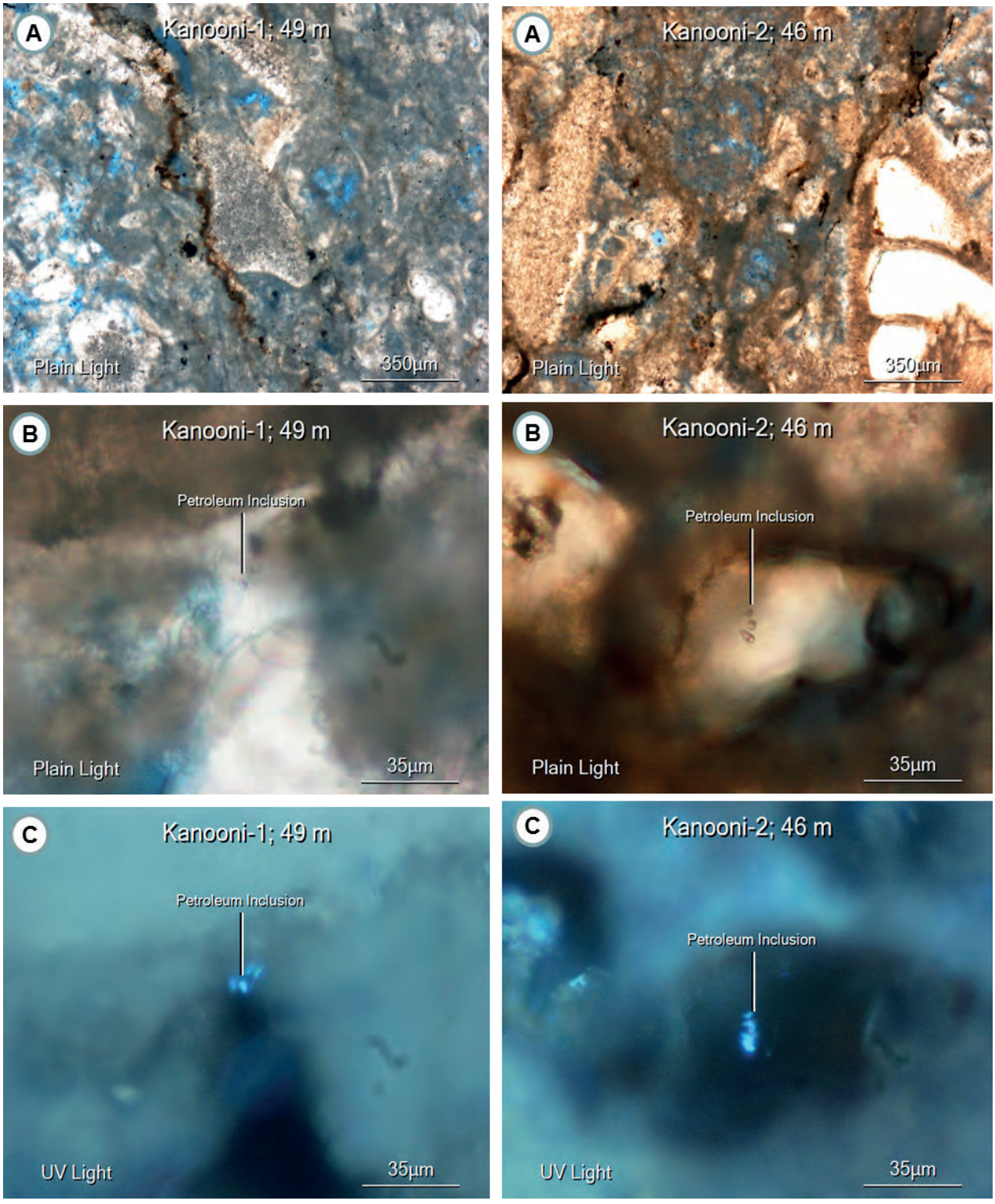

Fig. 10. A-C (left column) several white fluorescent, unknown gravity oil inclusions in bioclastic foraminiferal grainstone microfacies, Dahra Formation, Well no. 8 (3229 ft / 985 m); A-C (right column) several to common occurrences of blue fluorescent, unknown gravity petroleum inclusions in porous bioclastic foraminiferal grainstone microfacies, Dahra Formation, Well no.9 (3216 ft / 980 m).

mosaic took place in the near-surface meteoric zone from freshwater. Pre-compaction patchily-distributed equant sparry calcite and the early stage of syntaxial cement overgrowth around echinoderm grains were probably also precipitated in the meteoric zone, but in the phreatic part. Under cathodoluminescence, the meteoric cements are generally non-luminescent to dull (weakly)

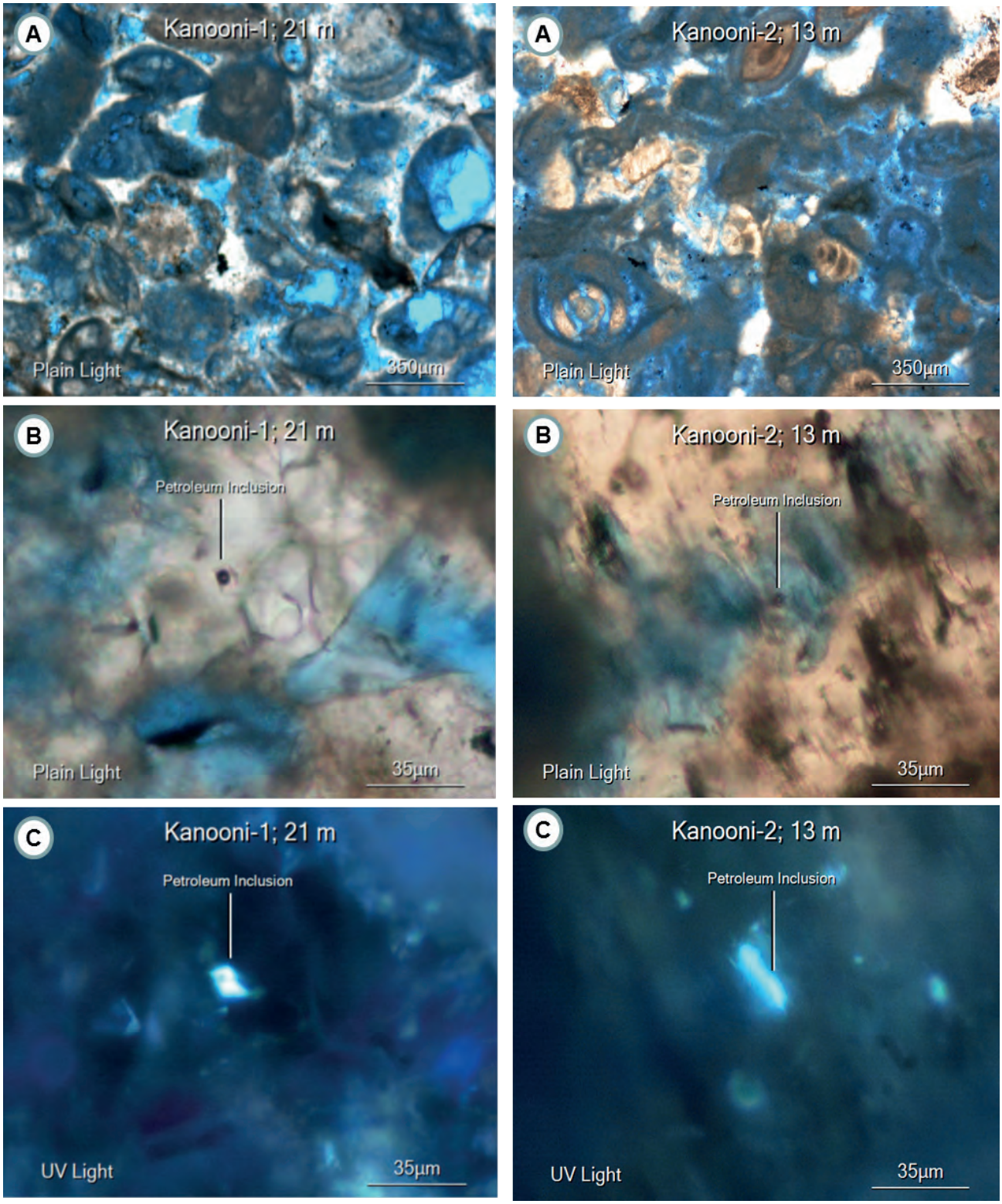

Fig. 11. A-C (left column) abundance of yellow fluorescent, unknown gravity oil inclusions in porous bioclastic wackestone/ packstone microfacies, Zelten Fm, Well no. 8 (2788 ft / 850 m); A-C (right column) rare to several white fluorescent, unknown gravity oil inclusions in dolomitic bioturbated bioclastic packstone microfacies, Harash Fm, Well no.9, (2698 ft / 820 m).

luminescent. There is some indication of subaerial exposure and pedogenesis in the form of desiccation cracks, fenestrae and rootlets in a dolomitic, brecciated and mottled fabric, in the Dahra Formation and lower part of the Zelten Formation.

In the deeper burial environment, the precipitation of coarse ferroan calcite and dolomite cements, fracturing, and formation of pressure

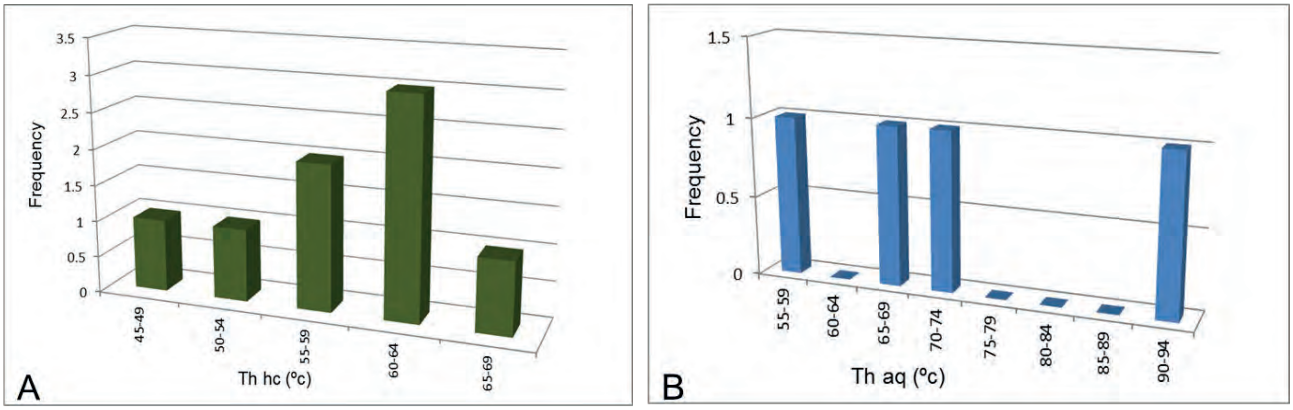

Fig. 12. Homogenization temperature of petroleum inclusions (A) and aqueous inclusions (B) against frequency in the Selandian / Thanetian succession (Harash, Zelten and Dahra Formations).

Diagenetic Processes		Diagenetic Environments		Time →
		Marine	Meteoric	Burial
Micritization & boring				
Isopachous rim cement				
Dissolution				
Cementation	Equant sparry calcite			
	Meniscus cement			
	Syntaxial rim			
	Coarse calcite			
Compaction	Physical			
	Chemical			
Dolomitization	V. fine to medium			
	Coarse dolomite			
Fracturing				
Hydrocarbon entry				

Fig. 13. Main diagenetic events and environments of the Selandian/Thanetian carbonates in the study area.

dissolution seams and stylolites were the main processes affecting the Selandian/Thanetian carbonates. The medium to coarsely crystalline dolomite has two luminescence characters; inner weakly to non-luminescent and thin outer slightly bright orange zones, indicating precipitation during a time of changing pore-fluid chemistry. The homogenisation temperatures of both petroleum inclusions and aqueous inclusions could indicate two phases of burial calcite precipitation. There is clear petrographic evidence for dissolution having taken place in the burial environment, especially of coarse dolomite crystals and the muddy-matrix between grains. On the whole, burial diagenetic processes have affected these carbonates much more than near-surface, eogenetic processes.

Porosity and Permeability Distribution in the Selandian/Thanetian Carbonates

The two main reservoir parameters (porosity and permeability) of the Paleocene succession are discussed following core sample (hand specimen)

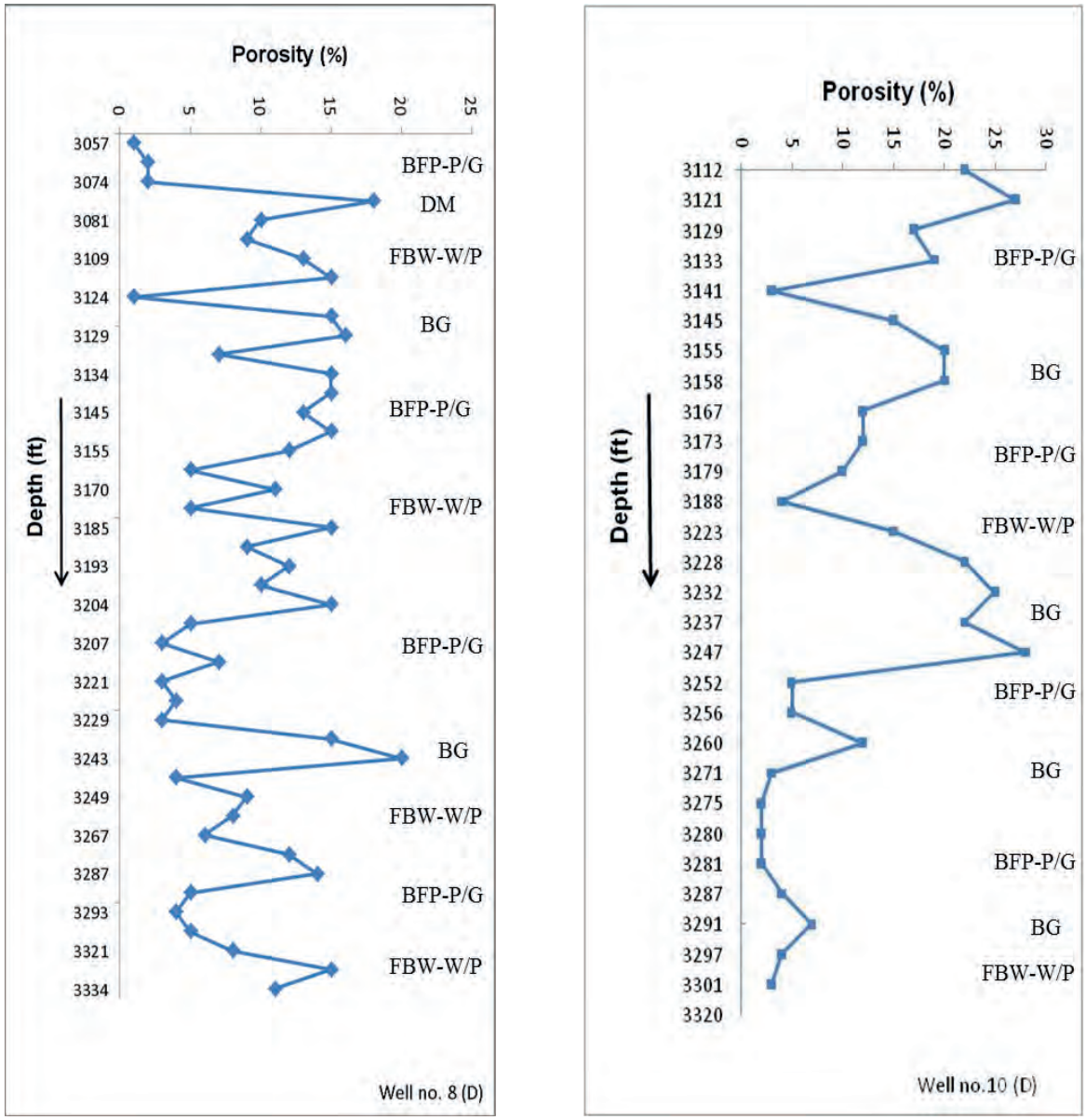

Fig. 14. Depth-porosity (observed) relationship for the cored section of the Dahra Formation in Well no. 8 (A) and Well no. 10 (B). The facies types are also shown.

inspection, thin-section observations, core analysis results, and scanning electron microscope examination.

The Dahra Formation: Macroscopic and microscopic investigations reveal that the porosity types developed in the Dahra platform carbonates are dominated by moldic, vuggy, intergranular and intragranular types, with less common fracture and intercrystalline porosity (Figs. 3, 5C & D, 6C). The porous layers are separated locally by thin beds of shale and marl/argillaceous limestone that act as porosity and permeability barriers; these compartmentalise the formation into several major reservoir units.

The best primary porosity is developed in bioclastic grainstone and bioclastic foraminiferal packstone-packstone/grainstone facies, where it reaches up to 10%. The intragranular type of porosity is commonly developed within both the skeletal and non-skeletal carbonate grains, in particular foraminifera and coated grains. Intergranular porosity appears to have provided pathways for undersaturated fluids to pass through the sediment

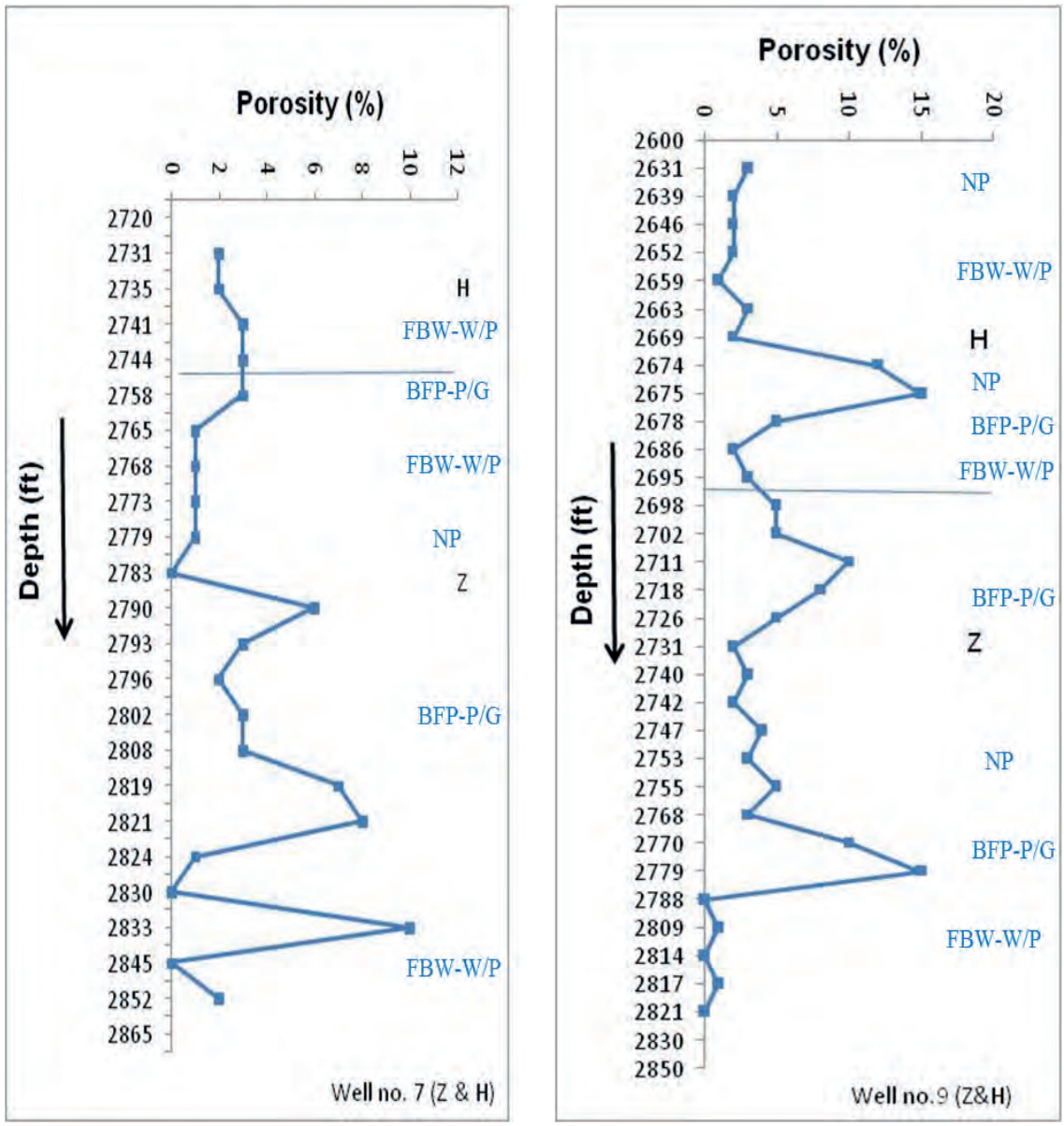

Fig. 15. Depth/porosity (observed) relationship of the cored section of Zelten (Z) / Harash (H) Formations in Well no.7 (A) and Well no. 9 (B).

and thus create secondary dissolution porosity (Figs. 5C & 6C). The low primary porosity of most facies is attributed mainly to the quite muddy (lime mud) nature of many units and the precipitation of equant calcite, Fe-rich calcite, dolomite and syntaxial rim cements in more grainy facies (Figs. 3E, 5F, 6A).

Intercrystalline porosity occurs wherever dolomite is present, in completely dolomitised facies and, less importantly, in partially dolomitic limestone facies. It is the main porosity type, along with moldic, in the dolomitic mudstone facies (Fig. 6C). Dolomite-dominated intervals are relatively thin in relation to limestone-dominated units; they generally have fair to good porosity even in the mud-supported layers, reaching 20% in some cases. This is probably related to dolomitization leading to an increase in crystal size, an increase in pore volume due to a net addition of dolomite, the development of moldic pores and an increasing resistance to compaction (Lucia, 1999).

Dissolution porosity is widespread in the Dahra Formation and occurs in many facies in different proportions, and usually in association with primary inter- and intra-granular porosity. Its highest value

occurs in grain-supported facies, where it reaches 15%. Fracture porosity has developed locally within the Dahra Formation and is well developed in some wells. A network of open microfractures that were connected to each other developed notably within marl/argillaceous limestone intervals.

Microporosity is also present in the Dahra Formation, particularly in Wells no. 8 and 9, and occurs as intercrystalline micro-voids between subhedral to anhedral micrite, microsparite and/or dolomite crystals (Fig. 5B). It is usually moderately connected through relatively narrow pore-throats, but locally it is almost completely isolated. Thus, its contribution to reservoir quality is likely insignificant. The best observed porosity in the Dahra Formation is within the bioclastic foraminiferal packstone/grainstone facies in almost all of the examined wells. It is averaging 20-25% in Well no. 9, and 15-20% in Well no. 8. This is probably related to meteoric influence during minor sea-level fluctuations. Increased porosity near the top of the Dahra Formation may be related to uplift and meteoric exposure during the Mid Tertiary. There is no apparent relation between observed porosity and depth (Fig. 14), suggesting that porosity evolution was controlled by the original depositional texture and subsequent diagenetic alterations (Fig. 4).

The Zelten and Harash Formations: The thin-section porosity in the Zelten/Harash interval is generally low, particularly in the Harash Formation (Fig. 15). The Zelten Formation, however, has marginally better porosity, especially in the grain-dominated facies, where the best porosity is developed in the bioclastic foraminiferal packstone-packstone/grainstone and, less important, foraminiferal nummulitic packstone facies. Porosity reaches 20%, especially in Well no. 10. A notable feature is that the least estimated porosity in the grain-supported facies is mostly recorded where echinoderm fragments are relatively common. This is probably the result of overgrowth cements around echinoderms, which can grow faster than finer, polycrystalline cements.

There is no clear relationship between the observed porosity and depth within the Zelten/Harash succession (Fig. 15). The low reservoir quality is due to the presence of mud-supported facies throughout the cored interval, the occurrence of argillaceous material within the grain-supported facies, fairly extensive compaction, and less important calcite cementation.

CONCLUSIONS

The Dahra, Zelten and Harash formations in the western Sirt Basin, Libya, contain units which are significant hydrocarbon reservoirs. They are mainly composed of bioclastic, especially foraminiferal carbonates with minor amounts of shale. They were deposited on a platform with a marginal homoclinal ramp towards the basin in the west. Inner, mid and outer ramp facies are recognised, each with distinctive microfacies. After the Dahra Formation, a phase of terrigenous mud deposition across the basin (Khalifa Shale) was followed by the Zelten and Harash formations with local occurrences of nummulitic packstone, in a mainly wackestone-packstone succession.

Different types of calcite and dolomite cements occur within the Late Paleocene succession and dissolution took place at various stages in the sediment's history from near-surface to burial. For the most part the diagenesis of the ramp carbonates is dominated by burial compaction and cementation, with minor marine-meteoric effects. The low positive $\delta^{13}C$ trend varying little through the succession reflects near-constant seawater $\delta^{13}C$ and primary marine signatures in the carbonates, and thus, a lack of diagenetic alteration involving organic matter. The presence of positive $\delta^{18}O$ values within the upper Dahra Formation coinciding with finely crystalline dolomite, suggests early dolomitization through circulating seawater. This contrasts with zones of negative $\delta^{18}O$ and the variable values of the Zelten-Harash formations which reflect meteoric influences and/or the effect of increased temperature during burial and calcite cementation-neomorphism.

The porosity types developed in the Selandian/Thanetian succession are dominated by moldic, vuggy, intergranular and intragranular types, with less common fracture and intercrystalline porosity. Overall, the porosity evolution in the Selandian/Thanetian succession is controlled by original depositional texture and subsequent diagenesis.

ACKNOWLEDGEMENTS

We would like to express our sincere thanks to Libyan Petroleum Institute (LPI), who sponsored this study and to Department of Earth Science at Durham University, where the study has been conducted.

REFERENCES

Abadi, A. M. (2002). Tectonics of the Sirte Basin. *Unpublished PhD Dissertation*, Vrije Universiteit, Amsterdam ITC. Enschede, 187p.

Abadi, A. M.; Van Wees, J-D.; Van Dijk, P. M., Cloetingh, S. A. P. L. (2008). Tectonics and Subsidence Evolution of the Sirt Basin, Libya. *AAPG Bulletin, **92***: 993-1027.

Abdunaser, K. M. (2015). Review of the Petroleum Geology of the Western Part of the Sirt Basin, Libya**.** *Journal of African Earth Sciences, **111***: 76-91.

Abdunaser, K. M.; McCaffrey, K. J. W. (2014). Rift Architecture and Evolution: The Sirt Basin, Libya: The influence of Basement Fabrics and Oblique Tectonics. *Journal of African Earth Sciences **100***: 203–226.

Adams, A. E.; Mackenzie, W. S. and Guilford, C. (1984). Atlas of Sedimentary Rocks Under the Microscope. Longman, 104p.

Anketel, J. M. (1996). Structural History of the Sirt Basin and its Relationship to the Sabratah Basin and Cyrenaican Platform, Northern Libya. In: *The Geology of the Sirt Basin* (Edit. by: M. J. Salem; M. T. Busrewil; A. A. Isallati and M. A. Sola), Amsterdam, Elsevier ***3***: 57–87.

Barnett, A. J.; Wright, V. P.; Chandra, V. S. and Jain, V. (2015). Distinguishing Between Eogenetic, Unconformity-Related and Mesogenetic Dissolution: a Case Study from the Panna and Mukta Fields, Offshore Mumbai, India. *Geological Society, London, Special Publication*: 435p.

Barr, F. T. and Weegar, A. A.(1972). Stratigraphic Nomenclature of The Sirte Basin, Libya. 179 p. *Petrol. Explor. Soc. Libya*, Tripoli.

Bernaola, G.; Martín-Rubio, M. and Baceta, J. I. (2009). New High Resolution Calcareous Nannofossil Analysis Across the Danian/Selandian Transition at the Zumaia Section: Comparison with South Tethys and Danish Sections. *Geologica Acta, **7***: 79-92.

Chandra, V.; Wright, P.; Barnett, A.; Steele, R.; Milroy, P.; Corbett, P.; Geiger, S. and Mangione, A. (2015). Evaluating the Impact of a Late-Burial Corrosion Model on Reservoir Permeability and Performance in a Mature Carbonate Field Using Near-Wellbore Upscaling. *Geological Society,* London, *Special Publication **406***: 427-445.

Dickson, J. A. D. (1965). A Modified Staining Technique for Carbonate in Thin Section. *Nature*, 205-587.

Dunham, R. J. (1962). Classification of Carbonate Rocks According to Depositional Texture. In: Classification of Carbonate Rocks (Edit. by: Ham, W. E.). *Am. Assoc. Petr. Geo.s Bulletin, Memoir 1*: 108-171.

Ebner, M.; Piazolo, S.; Renard, F. and Koehn, D. (2010). Stylolite Interfaces and Surrounding Matrix Material: Nature and Role of Heterogeneities in Roughness and Microstructural Development. *Jou. Structural Geo., **32***: 1070-1084.

Ehrenberg, S. N.; Walderhaug, O. and Bjorlykke, K. (2012). Carbonate Porosity Creation by Mesogenetic Dissolution: Reality or Illusion. *BAAPG, **96***: 217-233.

El Hefnawi, M. A.; Mashaly, A. O.; Shalaby, B. N.and Rashwan, L. A. (2010). Petrography and Geochemistry of Eocene Limestone from Khashm Al-Raqaba Area, El-Galala El-Qibliya, Egypt. *Carbonates & Evaporites, **25***: 193-202.

Elton , H.; Abdullatif, O.; Makkawi, M.; Al-Ramadan, K. and Abdulraziq, A. (2015). Porosity Evolution Within High-Resolution Sequence Stratigraphy and Diagenesis Framework: Outcrop Analog of the Upper Jurassic Arab-D Reservoir, Central Saudi Arabia. *Arabian Journal of Geosciences, **8***: 1669-1690.

Embry, A. F. and Klovan, J. E. (1971). A Late Devonian Reef Tract on Northeastern Banks Island, Northwest Territories. *Bull. Can. Petrol. Geol., **19***: 730 - 781.

Flügel, E. and Munnecke, A. (2010). *Microfacies of Carbonate Rocks: Analysis, Interpretation and Application.* **2nd edn**. Springer-Verlag, Berlin, 984 p.

Folk, R. L. and Lynch, F. L. (2001). Organic Matter, Putative Nanobacteria and the Formation of Ooids and Hardgrounds. *Sedimentology, **48***: 215-229.

Gingras, M. K.; Pemberton, S. G.; Muelenbachs, K. and Machel, H. (2004). Conceptual Models for Burrow-Related, Selective Dolomitization with Textural and Isotopic Evidence from the Tyndall Stone, Canada. *Geobiology, **2***: 21–30.

Green M. A. and Aller, J. Y. (1992). Experimental Evaluation of the Influences of Biogenic Reworking on Carbonate Preservation in Nearshore Sediments. *Marine Geology, **107***: 175–181.

Gumati, Y. D. (1982). Paleocene Facies of the Sirte Basin and Structural Evolution of the Basin During Paleocene Time: *Master's Thesis*, University of South Carolina, Columbia, South Carolina: 55p.

Gumati, Y. D. and Nairn, A. E. (1991). Tectonic Subsidence of the Sirt Basin, Libya. *Jour. Pet. Geol., **14***: 93–102.

Gumati, Y. D. and Schamel, S. (1988). Thermal Maturation History of the Sirte Basin, Libya: *Jour. Pet. Geol., **11***: 205–218.

Hallett, D. (2002). *Petroleum Geology of Libya*. Elsevier, Amsterdam. 503 p.

Have T. Ten, Heijnen W. (1985). Cathodoluminescence Activation and Zonation in Carbonate Rocks: An Experimental Approach. *Geol Mijnbouw, **64***: 297–310.

Hillgärtner, H.; Dupraz, C. and Hug, W. (2001). Microbially Induced Cementation of Carbonate Sands: are Micritic Meniscus Cements Good Indicators of Vadose Diagenesis? *Sedimentology, **48***: 117–131.

James, N. P. and Jones, B. (2015). Origin of Carbonate Sedimentary Rocks. American Geophysical Union & John Wiley, Chichester.

Koch, P. L.; Clyde, W. C.; Hepple, R. P.; Fogel, M. L.; Wing, S. L. and Zachos, J. C. (2003). Carbon and Oxygen Isotope Records from Paleosols Spanning the Paleocene-Eocene Boundary, Bighorn Basin, Wyoming. In: Causes and Consequences of Globally Warm Climates in the Early Paleogene.Geol (Edit. by: Wing, S. L., Gingerich, P. D., Schmitz, B. and Thomas, E.) *Soc.* Am. Spec. Publ., ***369***: 49-64.

Logan, B. W. and Semniuk, V. (1976). Dynamic Metamorphism; Process and Products in Devonian Carbonate Rocks: Canning Basin, Eastern Australia. Western Australia. *Geol. Soc. Australia, Spec. Publ., **6***: 138-150.

Longman, M. W. (1980). Carbonate Diagenetic Textures from Near-Surface Diagenetic Environments. *Bull. Am. Ass. Petrol. Geol., **64***: 461-487.

Lucia, F. J. (1999). *Carbonate Reservoir Characterization*. Springer-Verlag Berlin Heidelberg, 226 p.

Machel, H. G. and Burton, E. A., (1991). Factors Governing Cathodoluminescence in Calcite and Dolomite. In: Luminescence Microscopy: Quantitative aspects (Edit. by: Barker, C. E and Kopp, D. C.). *Soc. Econ. Paleont. Miner, Short Course, **25***: 37-57.

Madden, R. H. C. and Wilson, M. E. J. (2013). Diagenesis of a SE Asian Cenozoic Carbonate Platform Margin and its Adjacent Basinal Deposits. *Sedimentary Geology, **286-287***: 20–38.

Mazzulo, S. and Harris, P. M. (1992). Mesogenetic Dissolution: its Role in Porosity Development in Carbonate Reservoirs. *BAAPG, **76***: 607-620.

Miller, K. G.; Kominz, M. A.; Browning, J. V.; Wright, J. D.; Mountain, G. S.; Katz, M. E.; Sugarman, P. J.; Cramer, B. S.; Christie-Blick, N. and Pekar, S. F., (2005). The Phanerozoic record of global sea-level change. *Science, **310***: 1293-1298.

Morgan, W. J. (1980). Hot-Spot Tracks and the Opening of the Atlantic and Indian Oceans. In: *The Sea* (Edit. by: C. Emiliani) Wiley, New York, ***V. 7***: 443-467.

Morgan, W. J. (1983). Hot-Spot Tracks and the Early Rifting of the Atlantic. *Tectonophysics, **94***: 123-139.

Mouzughi, A. J. and Taleb, T. M. (1982). Tectonic elements of Libya (1:2 000 000). National Oil Corporation, Libya.

Nader, F. H.; Swennen, R. and Keppens, E. (2008). Calcitization/Dedolomitization of Jurassic Dolostones (Lebanon): Results from Petrographic and Sequential Geochemical Analyses. *Sedimentology, **55***: 1467-1485.

Pujalte, V.; Orue-Etxebarria, X.; Schmintz, B.; Tosquela, J.; Baceta, J. I.; Payros, A.; Bernaola, G.; Caballero, F. and Apelleniz, E. (2003). Basal Ilerdian (Earliest Eocene) Turnover of Larger Foraminifera: Age Constraints Based on Calcareous Plankton and 8I3C Isotopic Profiles from New Southern Pyrenean Sections (Spain). *Geol. Soc. America, Special Paper, **369***: 205-221.

Rameil, N. (2008). Early Diagenetic Dolomitization and Dedolomitization of Late Jurassic and Earliest Cretaceous Platform Carbonates: A Case Study from the Jura Mountains (NW Switzerland, E France). *Sedimentary Geology, **212***: 70-85.

Ruban, D. A.; Zorina, S. O. and Conrad, C. P. (2010). No Global-Scale Transgressive-Regressive Cycles in the Thanetian (Paleocene): Evidence from Interregional Correlation. *Palaeogeography, Palaeoclimatology, Palaeoecology, **295***: 226-235.

Ruban, D. A.; Zorina, S. O.; Conrad, C. P. and Afanasieva, N. I., (2012). In Quest of Paleocene Global-scale Transgressions and Regressions: Constraints from a Synthesis of Regional Trends. *Proceedings of the Geologist's Association, **123***: 7-18.

Rustichelli, A.; Tondi, E.; Korneva, I.; Baud, P.; Vinciguerra, S.; Agosta, F.; Reuschlé, T. and Janiseck, J. M. (2015). Bedding-Parallel Stylolites in Shallow-Water Limestone Successions of the Apulian Carbonate Platform (Central-Southern Italy). *Italian Journal of Geoscience, **135DOI***: 10.3301/IJG.2014.35.

Swati, M. A. F.; Haneef, M.; Ahmad, S.; Latif, K.; Naveed, Y.; Waseem Zeb, W.; Akhtar, N. and Owais, M. (2014). Diagenetic Analysis of the Early Eocene Margala Hill Limestone, Pakistan. *Journal of Himalayan Earth Sciences, **47***: 49-61.

Tucker, M. E. (1993). Carbonate Diagenesis and Sequence Stratigraphy. In: *Sedimentology Review* (Edit. by: V. P. Wright), ***1***: 51-72. BlackWell Science, Oxford.

Tucker. M. E. and Wright, V. P. (1990). *Carbonate Sedimentology.* BlackWell Science, Oxford, 482p.

Van Berk, W.; Yunjiao Fu, Y. and Schulz, H. M. (2015). Creation of Pre-Oil-Charging Porosity by Migration of Source-Rock-Derived Corrosive Fluids Through Carbonate Reservoirs: One-Dimensional Reactive Mass Transport Modelling. *Petroleum Geoscience, **21***: 35-42.

Van der Meer, F. and Cloetingh, S. (1996). Intraplate Stresses and the Subsidence History of the Sirt Basin. In: *First Symposium on the Sedimentary Basins of Libya, Geology of the Sirt Basin* (Edit. by: M. J. Salem, M. T. Busrewil, A. A. Misallati, and M. J. Sola), Elsevier, ***V. 3***: 211-230. Amsterdam

Volery, C.; Davaud, E.; Foubert, A. and Caline, B. (2009). Lacustrine Microporous Micrites of the Madrid Basin (Late Miocene, Spain) as Analogues for Shallow-Marine Carbonates of the Mishrif Reservoir Formation (Cenomanian to Early Turonian, Middle East): *Facies, **56***: 385-397.

Wong P. K. and Oldershaw, A. E. (1981). Causes of Cyclicity in Reef Interior Sediments, Kaybob Reef, Alberta. *Bull. Can. Petrol. Geol., **28***: 411-424.

Wright, V. P. and Harris, P. M. (2013). Carbonate Dissolution and Porosity Development in the Burial (Mesogenetic) Environment. *AAPG*, Search & Discovery article ***# 50860***.

Zachos, J. C.; Schouten, S.; Bohaty, S.; Quattlebaum, T.; Sluijs, A.; Brinkhuis, H.; Gibbs, S. J. and Bralower. T. J. (2006). Extreme Warming of Mid-Latitude Coastal Ocean During the Paleocene-Eocene Thermal Maximum: Inferences from TEX86 and Isotope Data. *Geology, **34***: 737-740.

Zeff, M. L. and Perkins, R. D. (1979). Microbial Alteration of Bahamian Deep-Sea Carbonates. *Sedimentology, **26***: 175-201.

Zenger, D. H. (1992). Burrowing and Dolomitization Patterns in the Steamboat Point Member, Bighorn Dolomite (Upper Ordovician), Northeast Wyoming. *Contributions to Geology, **29***: 133-142.

ABOUT THE AUTHORS

Ibrahim Elkanouni is a senior geologist (Associate Researcher) in the Exploration Department at Libyan Petroleum Institute (LPI). He has got an MSc degree from University of Manchester and PhD from Durham University, UK.

He is specialist in carbonate sedimentology and sequence stratigraphy and has been involved in several studies concerning Libyan sedimentary basins and oil fields, in onshore and offshore regions, studied carbonates from Paleozoic, Mesozoic and Cenozoic successions. Has supervised the sedimentology research group at Libyan Petroleum Institute (2002-2009). He has been teaching at Geology Department, University of Tripoli since 2002.

Maurice Tucker is a visiting professor at the University of Bristol and emeritus professor at Durham University since 2011, after nearly 30 years at Durham, after positions at Newcastle, UC Berkeley, Cardiff and Sierra Leone. His interests are in limestones, their deposition, diagenesis, reservoir potential and he has studied carbonates from most geological periods from many parts of the world. He has published over 150 papers and written several books including Sedimentary Petrology (2000), Sedimentary Rocks in the Field (2011), Carbonate Sedimentology (with Paul Wright, 1990), and Petrologia Sedimentar Carbonatica (with Dimas Dias-Brito, 2017). His current interest is in viruses and their role in carbonate precipitation: viruses are the new role in Earth Science.